DE GRUYTER Open Chemistry 2024; 22: 20240026

**Research Article**

Yousaf Khan, Muhammad Naeem Khan, Abdul Salam, Haleema Sadia, Muhammad Farhat Ullah, Muhammad Ijaz Khan*, Barno Sayfutdinovna Abdullaeva, Fuad A. Awwad, Emad A. A. Ismail

# Photocatalytic treatment of organic dyes using metal oxides and nanocomposites: A quantitative study

https://doi.org/10.1515/chem-2024-0026
received September 25, 2023; accepted April 5, 2024

**Abstract:** This comprehensive and quantitative research offers a thorough analysis of how metal oxides and nanocomposites are used in the photocatalytic treatment of organic dyes. It explores the challenges and opportunities of employing photocatalytic conversion technologies, discussing the optimal conditions for efficient degradation. The mechanisms of photocatalytic degradation are elucidated, highlighting the steps involved in transforming organic dyes into harmless by-products. Additionally, the article examines the factors that enhance the overall efficiency of photocatalytic conversion and compares its cost-effectiveness to other treatment methods. Various photocatalysts, with a focus on metal oxides and nanocomposites, are analyzed in terms of their advantages and limitations in degrading organic dyes. This article serves as a valuable resource for researchers and practitioners seeking sustainable and economical wastewater treatment solutions through efficient and eco-friendly photocatalytic approaches.

**Keywords:** nanotechnology, nanomaterials, photocatalysis, metal oxides, nanocomposites, organic dyes, quantitative results

## 1 Introduction

Water is an essential resource for human development and survival on Earth. It is indeed the basic need of all processes. Whether the users are domestic, industrial, commercial, or agricultural, they all need water for their proper functioning [1]. As a result of the industrial revolution and technological advancement, various new industries are on a global level. These industries also use water as a raw material and waste removal medium. Waste from such units contains toxic substances such as heavy metals, organic toxins, and solid organic wastes [2,3].

Furthermore, due to the population explosion, pure water needs have increased [4]. These factors, i.e., population explosion and industrialization, are significant causes of environmental pollution. Organic substances that are not even toxic are also an environmental hazard. For instance, the discharge of oil in water bodies results in lethal damage to the marine ecosystem. It causes deoxygenation in water and hypoxia in surroundings [5]. Pollutants in water are mainly of anthropogenic origin.

Based on the origin of pollutants, water pollution sources may be direct or indirect sources [6,7]. Fluids of different quality from industries, plants for waste treatment, refineries, etc., are direct sources of water contamination. Usually, the effluents are dumped into freshwater supplies. Water contaminations caused by air, soil, and sewerage systems are the indirect sources of water pollution. Polluted air contains oxides of nitrogen, sulfur, carbon, and greenhouse gases (chlorofluorocarbons), which are emitted from automobiles and industries [8]. These gases cause acid rain and toxify water. Soil pollutants include fertilizers, pesticides, industrial wastes, and domestic wastes. Rainwater

---

*** Corresponding author: Muhammad Ijaz Khan**, Department of Mechanics and Engineering Science, Peking University, Beijing 100871, China; Department of Mechanical Engineering, Lebanese American University, Beirut, Lebanon, e-mail: 2106391391@pku.edu.cn
**Yousaf Khan:** Dalian Institute of Chemical Physics, Chinese Academy of Sciences, Dalian, Liaoning, 116023, PR China
**Abdul Salam, Haleema Sadia:** Department of Chemistry, Quaid-i-Azam University, 45320, Islamabad, 44000, Pakistan
**Muhammad Naeem Khan:** Department of Chemistry and Chemical Engineering, Syed Babar Ali School of Science and Engineering, Lahore University of Management Sciences, Lahore, 54792, Pakistan
**Muhammad Farhat Ullah:** Genome Editing & Sequencing Lab, National Centre for Bioinformatics, Quaid-I-Azam University Islamabad, Islamabad, Pakistan
**Barno Sayfutdinovna Abdullaeva:** Doctor of Pedagogical Sciences, Vice-Rector for Scientific Affairs, Tashkent State Pedagogical University, Tashkent, Uzbekistan
**Fuad A. Awwad, Emad A. A. Ismail:** Department of Quantitative Analysis, College of Business Administration, King Saud University, P.O. Box 71115, Riyadh, 11587, Saudi Arabia

seeps through the polluted soil and carries the contaminants to the groundwater. Sewerage systems in urban areas are another indirect source of unclean water. This article mainly focuses on organic pollutant dyes and their photocatalytic degradation through various advanced metal oxide nanoparticles and nanocomposites.

Approximately 300–400 million tons of unprocessed organic pollutants are discharged annually, causing water contamination concerns, particularly near industrial regions [6,9]. Consequently, it is crucial to prioritize the improvement and innovation of environmentally friendly, energy-efficient, and cost-effective technologies for purifying water. To tackle the challenges, developing an innovative and economically viable technology that can effectively remove contaminants from wastewater with minimal energy consumption and chemical usage is essential. To address this need, researchers have directed their efforts toward advanced oxidation processes (AOPs) as reliable alternatives capable of oxidizing and mineralizing a wide range of organic chemicals due to their highly potent and strongly oxidizing radicals, such as hydroxyl radicals ($^{\cdot}OH$) and oxide radicals ($O_2^{\cdot -}$) [10]. AOPs employ an aqueous phase oxidation technique that harnesses the *in situ* generation of powerful oxidizing agents to accelerate the oxidation of water and wastewater contaminants [11,12]. AOPs have gained much interest because of their effectiveness in ultimately converting pollutants into less toxic compounds and their capacity to break down toxins quickly and without selectivity [13]. Chemical agents such as metals, $O_3$, or $H_2O_2$ are frequently used in these processes, as well as energy sources such as ultraviolet or visible light, ultrasound, electric current, or irradiation. Light-absorbing catalysts (photocatalysts) have demonstrated exciting uses in the degradation of poisonous dyes and the reduction of heavy metal ions to less hazardous forms in recent years. Photocatalysts offer higher catalytic efficiency, shorter reaction times, and the absence of dangerous secondary by-products. Under optimal conditions, solar energy can initiate photocatalysis through photons' absorption rather than relying on thermal energy. When exposed to UV light, several semiconductors are utilized in photocatalysis, producing highly energetic electron–hole pairs. These electron–hole pairs can generate reactive oxygen species, particularly $^{\cdot}OH$ and $O_2^{\cdot -}$ radicals, which possess strong oxidizing properties and can migrate to the outer surface, initiating oxidation and reduction reactions [14,15]. This article primarily focuses on degrading organic dyes using metal oxides and nanocomposites through photocatalysis.

## 2 Organic dyes and their classification

The sense of color comes from the brain's interpretation of the eye's stimulation by light. Because of this, color perception may vary based on the viewer. The pigments and dyes are tabulated into variants [16] such as colored, colorless, or fluorescent coloring agents. Pigments are often finely divided solids or powders that are insoluble in a dissolved solution. Dye is a colored soluble substance [17].

In contrast to pigments, where the physical characteristics of the particle (such as particle size and shape) correlate with the color of the pigment, dyes and chemical structures predetermine its color characteristics [18,19]. The primary distinction between dyes and pigments is solubility. Unlike dyes, which become soluble throughout their application procedures, pigments remain essentially insoluble during various application processes [20,21].

Organic dyes are compounds with a chromophore group that absorbs specific wavelengths of light and gives them their characteristic color. It is widely used in various applications, including textiles, food, and cosmetics. Organic dyes can be classified based on their chemical structure, application, and color properties. Here are some of the standard classifications of organic dyes [22]:

i. **Azo dyes:** Organic dyes with a nitrogen–nitrogen double bond are azo dyes (azo group). They are the most widely used dyes in the textile and food industry.
ii. **Anthraquinone dyes:** These are derived from anthracene, a hydrocarbon containing three fused benzene rings. They are commonly used to produce textiles, paper, and plastic colorants.
iii. **Phthalocyanine dyes:** Phthalocyanine dyes are synthetic organic dyes containing a phthalocyanine ring. They are widely used in the production of inks and pigments.
iv. **Triarylmethane dyes**: They have a central carbon atom bonded to three aryl groups. They are commonly used in the production of colored paper, textiles, and ink.
v. **Acid dyes:** Acid dyes are water-soluble dyes primarily used for dyeing wool, silk, and nylon. They are typically used in the production of clothing, carpets, and other textiles.
vi. **Basic dyes:** Water-soluble dyes are often used to color acrylic fibers, paper, and leather. They are also used as biological stains in medical and research laboratories.
vii. **Direct dyes:** Direct dyes are water-soluble dyes mostly used to color cotton, silk, and other cellulosic fibers.

They are commonly used in the production of clothing and home textiles.

viii. **Reactive dyes:** Cellulosic fibers like cotton and rayon are colored with a type of dye known as a reactive dye, a variety of water-soluble dye. They are utilized frequently in the textile sector and are famous for the brilliant eye-catching colors that they produce.

These are just a few examples of the various types of organic dyes and their classifications. The color and characteristics of dye molecules depend on their chemical structure [23]. As a result, they can be divided into categories based on their chemical composition (functional groups), color, or use characteristics. Acid, basic, direct, azo, naphtha, reactive, mordant, vat, dispersion, and sulfur dyes are among the variants often used in the textile industry; at the moment, azo dyes are the most popular [24,25]. Dyes are often categorized using their molecular charge following dissociation in aqueous-based applications to research their characteristics regarding photo-degradation processes [26]. In Tables 1–3, the chemical structures of several typical dyes widely applied in photo-degradation applications are shown. Based on their chemical structure, they are divided into cationic, neutral, and anionic dyes [26,27].

## 3 Wastewater treatment

Dyes are organic and hence are rendered as impurities [41]. They produce perilous by-products in wastewater via oxidation, hydrolysis, and other chemical reactions [42]. The question arises: at what concentration do these

**Table 1:** Anionic dyes [28–33]

| Commercial name | Structure | Mol. wt. (g/mol) | $\lambda_{max}$ (nm) | Supplier |
|---|---|---|---|---|
| Acid red 151 | 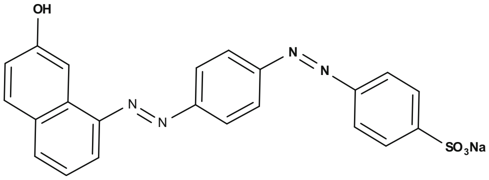 | 454 | 512 | Sigma-Aldrich |
| Acid orange 7 | 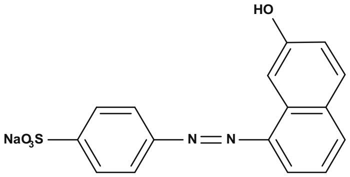 | 350 | 483 | Boruta, Poland |
| Acid yellow 36 | 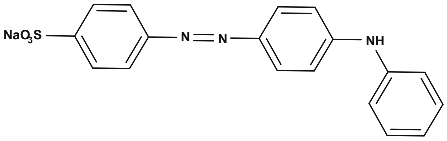 | 375 | 435 | Boruta, Poland |
| Methyl orange | 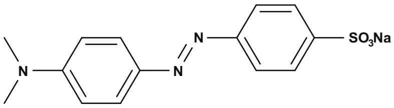 | 327 | 465 | Acros Organics |
| Orange G | 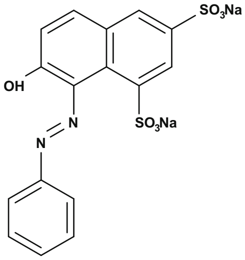 | 452 | 479 | Sigma-Aldrich |
| Alizarin yellow R | 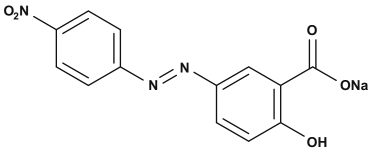 | 309 | 385 | MP bio-medicals |

**Table 2:** Neutral dyes [30,34–38]

| Commercial name | Structure | Mol. wt. (g/mol) | $\lambda_{max}$ (nm) | Supplier |
|---|---|---|---|---|
| Neutral red | 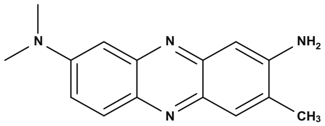 | 289 | 543 | Merck |
| Eosin-MB | 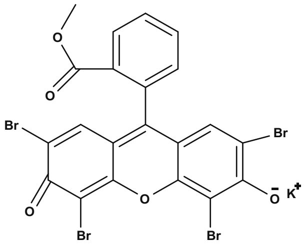 | 661 | 655 | Sigma-Aldrich |
| Giemsa's stain | 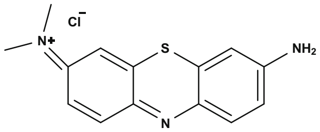 | 292 | 650 | SRL, India |
| Sudan III | 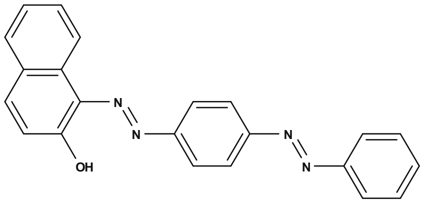 | 352 | 512 | Sigma-Aldrich |
| Oil red O | 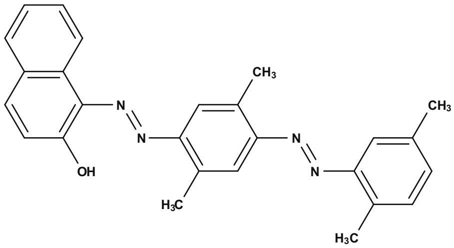 | 409 | 520 | Loba Chemie, India |
| Mordant violet 5 | 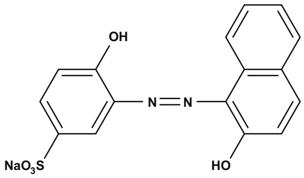 | 366 | 590 | Merck |

dyes pose a risk to life and aquatic life? The textile industries significantly contribute to aqua pollution [43,44]. They cause skin sensitization, respiratory and heart problems, and irritation; therefore, their disposed water must be treated per health standards [43,45]. Figure 1 highlights wastewater treatment, sources, and problems caused by polluted water.

Among the treatment methods, the best one is where complete mineralization of the organic components takes place without leaving any harmful by-product at all [46]. These methods include biological, chemical, physical, and AOPs [47–50]. The type of pollutant and the permitted contamination levels are used to determine which approach is most appropriate. Reducing contamination in industrial discharge and improving the use of treated water in sectors like the petrochemical and building industries are two main drivers for water treatment. Cost-effectiveness is another factor affecting the treatment method choice [51].

## 3.1 Conventional wastewater treatment technology and its drawbacks

Several methods have been reported to treat wastewater. These methods are broadly classified into three categories.

Table 3: Cationic dyes [30–32,39,40]

| Commercial name | Structure | Mol. wt. (g/mol) | $\lambda_{max}$ (nm) | Supplier |
|---|---|---|---|---|
| Crystal violet | 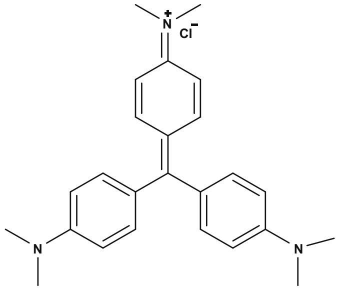 | 408 | 595 | Sigma-Aldrich |
| MB | 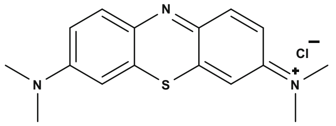 | 320 | 665 | Sigma-Aldrich |
| Rhodamine B | 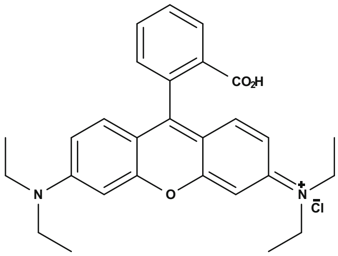 | 479 | 554 | Sigma-Aldrich |
| Astrazon orange G | 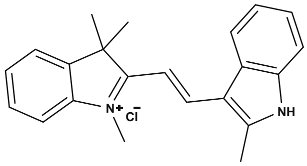 | 351 | 492 | Santa Cruz, USA |
| Nile blue A | 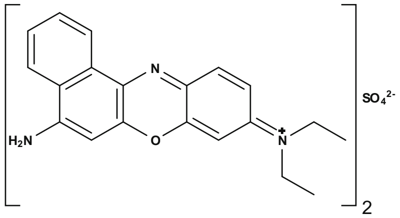 | 733 | 639 | Sigma-Aldrich |

### 3.1.1 Biological methods

Implementing biological methods has garnered recognition as viable and profitable solutions and environmentally friendly alternatives to conventional industrial wastewater treatment practices. These innovative processes use diverse natural agents, including microorganisms, bacteria, fungi, yeasts, algae, and enzymes, to facilitate biodegradation. Using these microbial and enzymatic activities, aerobic, anaerobic, or combined processes, ensures the efficient breakdown and elimination of pollutants in the wastewater, ultimately promoting a healthier and more sustainable ecosystem.

Biological methods have multiple requirements, and many factors act as limiting factors in this scenario. For instance, daytime variation, the toxicity level of pollutants, acidity, alkalinity, etc., many organic dyes are efficiently reduced by this method. Still, at the same time, sure others are highly unmanageable owing to their structure and synthetic origin. The chemical method employs several chemicals in the same flow, and the produced sludge further requires treatment. Due to these factors, it is a costly process.

### 3.1.2 Physical methods

The physical methods include membrane-based filtration processes and adsorption processes. The problem usually encountered in membrane-dependent operations is the

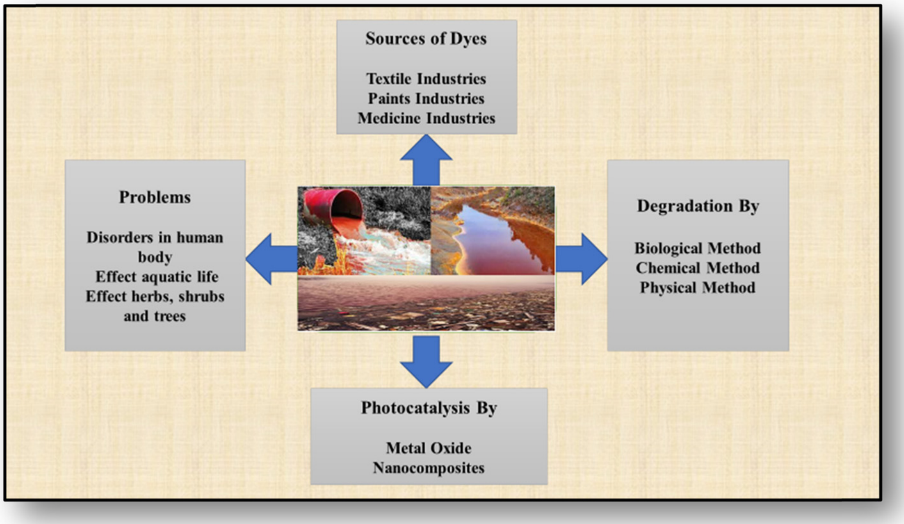

**Figure 1:** Wastewater treatment, sources, and problems caused by polluted water.

lifetime of the membrane. These cliché methods, although in industrial usage, are still ineffective in either completely removing the effluents from the water discharge or failing in removing the substances that are not readily absorbed to be removed.

### 3.1.3 Chemical methods

The chemical activities of OH are robust oxidation processes that remove hazardous organic molecules from the water. Every chemical purification technique used today uses dangerously strong oxidants or highly energetic ultraviolet radiation. Specific chemical refinement techniques, such as direct photolysis and the use of strong oxidants like $H_2O_2/O_3$/UV, $H_2O_2$/UV, and $O_3$/UV, can have a direct negative impact on the environment. Nonetheless, identifying running method parameters depends on the type of contamination present. Contemporarily, a relatively new technique is known as advanced oxidation. The process is promising because it reduces the organic components to $CO_2$ and $H_2O$. Table 4 indicates the significance of various techniques of dye degradation.

## 4 Photocatalysis

AOPs are promising techniques for wastewater treatment as they convert toxic organic substances into nontoxic components, i.e., water and carbon dioxide [1]. The term photocatalysis is formed by combining two words, photo and catalysis. A catalyst is a reagent that causes the chemical reaction to speed up by usually lowering the activation energy for the substrate. Furthermore, the catalyst has to be recovered at the end of the reaction. The photocatalyst is a substance that does the same but with the help of sunlight.

The best example in this regard is photosynthetic machinery. In the process, chlorophyll acts as the photocatalyst. Both photosynthesis and photocatalysis are analogous in function since both work as light-harvesting systems; chlorophyll absorbs the sunlight and converts water and carbon dioxide to glucose and oxygen. Similarly, photocatalysis yields strong oxidizing agents, transforming the organic matter into water and carbon dioxide in the presence of sunlight, water, and a catalyst, as depicted in Figure 2.

### 4.1 Photocatalysis for wastewater treatment

Recently, photochemical methods have been employed in the oxidative degradation of organic compounds. This method is particularly intriguing since it does not end in hazardous byproducts [57]. This method is generally known as an AOP. It is a highly recommended method by environmental activist agencies [58]. AOPs usually depend on oxygen-bearing intermediates such as superoxide ($O_2^{\cdot}$), hydroxyl radical (OH), and hydroperoxyl radicals (HOO) [59]. Intermediates are short-lived. The hydroxyl radical ($OH^{\cdot}$) is readily produced via

**Table 4:** Advantages and disadvantages of various methods of dye degradation

| Sr. No. | Methods | Advantages | Disadvantages | References |
|---|---|---|---|---|
| 1 | Biological method | Ease of maintenance, low preparation methods, inexpensive, readily available method, economic | Not consistently successful, unstable nature of enzymes, loss of activity, accumulation of biomass, long microbial accumulation, time-optimal degradation conditions challenging to establish | [52–54] |
| 2 | Physical method | Non-destructive, high-efficiency method, used for high concentration dyes, no by-products | It takes several hours and is a time-consuming method. Flux decline, membrane fouling in membrane technique | [55] |
| 3 | Chemical method | Economical reliable, environmentally friendly process, complete degradation of dyes, activation by solar energy use for both reduction and oxidation | Sometimes liberates unwanted harmful by-products | [17,56] |

ultraviolet light [60]. Furthermore, it is highly reactive and oxidizes the organic matter [61]. AOPs are more suitable for processes where saturated impurities are in excess. Such toxins are not oxidized via any other approach. AOPs include methods such as $H_2O_2$ in UV, $TiO_2$ in UV, $O_3$ in UV, $H_2O_2$ and $O_3$ in UV, and vacuum UV.

Some advantages of photocatalysis are as follows:

i. Organic matter such as $CC1_4$, which usually remains unaffected by the hydroxyl radical, is readily mineralized.
ii. The end products, i.e., water and carbon dioxide, have the most negligible environmental impact, hence the term green technology.
iii. This process uses atmospheric oxygen; no additional oxidants are needed.
iv. Photocatalysts are cost-effective, reusable, stable, and chemically and biologically inert.
v. The process is feasible under ultraviolet light for catalyst activation. Furthermore, it can work well under sunlight, too [62].

A myriad of features in semiconductors make them efficient photocatalysts. For photocatalysis, the semiconductor that acts as the photocatalyst is exposed to sunlight to generate a redox environment [63]. As a result of this irradiation, UV light absorption causes electrons in the valence band (VB) and holes in the conduction band (CB) [64]. The difference between the VB and CB is called the band gap ($E_g$) [65]. These generated electrons and holes can thus reduce and oxidize the organic and inorganic compounds [66]. For decades, since Fujishima and Honda's (1972) work on splitting water for creating hydro fuels using $TiO_2$ electrodes, semiconductors as photocatalysts have gained interest [67]. Ollis and Turchi suggested using semiconductors as photocatalysts in water purification [68]. Hence, the process only needs light and a photocatalytic semiconductor to achieve its purpose.

## 5 Principle of photocatalysis

Photocatalysis is the amalgam of two words: photochemistry and catalysis. It implies that for the occurrence of a chemical reaction, both light and catalyst are essential [69]. There is a massive difference between a photocatalytic and a mere catalytic reaction. In photocatalytic reactions, only light is the driving factor since it lowers the activation energy of the reaction. In contrast, conventional catalytic reactions use heat or other sources for this purpose. The light source generates electron–hole pairs, which play essential roles in the catalytic degradation of toxic dyes, as shown in Figure 3.

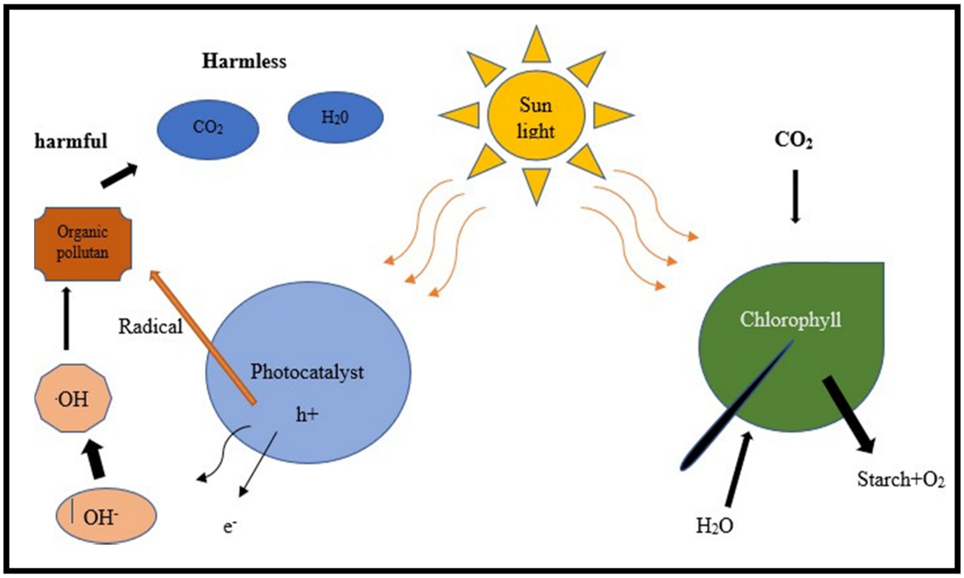

**Figure 2:** Photocatalyst and chlorophyll.

## 6 Types of photocatalysis

Based on differences in catalyst and substrate phases, photocatalysis is broadly classified into two categories.

### 6.1 Homogeneous photocatalysis

As the name predicts, homo means the same phase. In this case, both the catalyst and the substrate are in the same phase. This catalysis uses an intense UV lamp to illuminate the polluted water, whereas the catalysts commonly used are Fe, $O_2$, or $H_2O_2$ [70,71].

### 6.2 Heterogeneous photocatalysis

In this type of catalysis, both species are in different phases. In the process, electrons and holes are photo-generated on the catalyst's surface [72]. The reaction proceeds in more than one step. Compared to homogeneous photocatalysis, such reactions are challenging since the catalyst

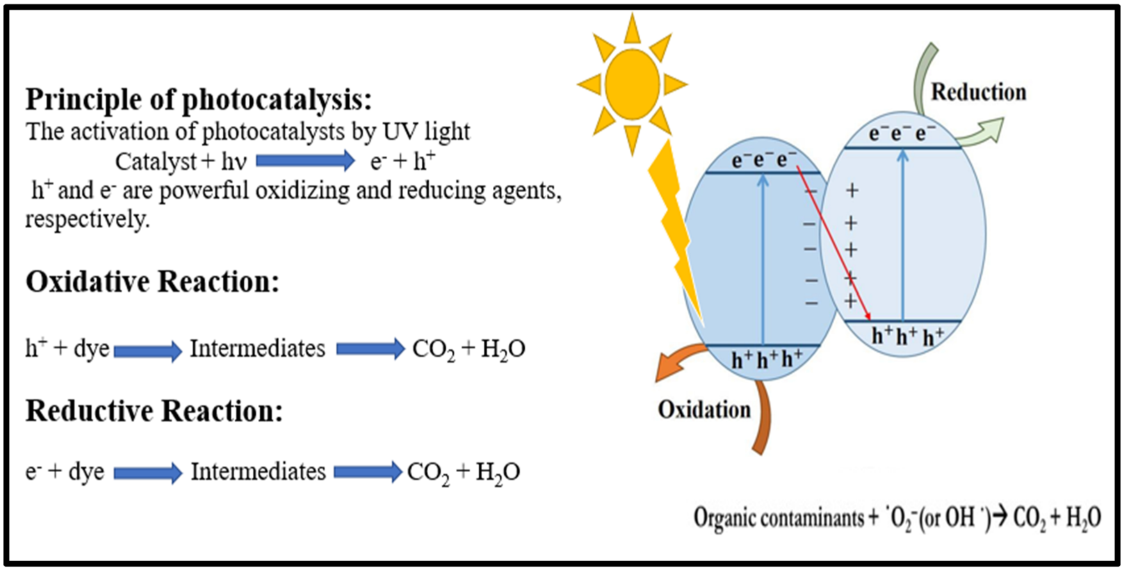

**Figure 3:** Principle of photocatalysis of organic dyes.

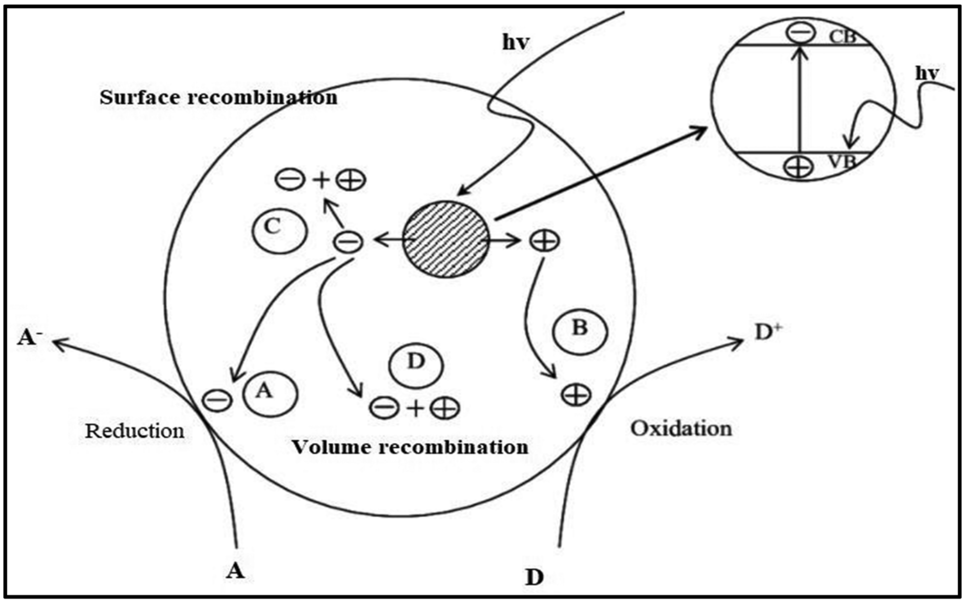

**Figure 4:** Schematic photoexcitation in a solid semiconductor.

is in a solid phase, while the substrate is in a liquid state. This review aims to look into heterogeneous photocatalysis-based organic pollutant degradation in aqueous media.

For heterogeneous photocatalysis, the redox reaction is facilitated by the photocatalyst. While choosing the semiconductor, specific properties are kept in view, such as the detailed electronic structure having an empty CB and filled VB [73]. With the absorption of a photon possessing band gap energy, the electron from the VB is promoted to CB, leaving a hole behind in the VB [74].

The lifetime of the photo-generated electrons and holes falls in the nanosecond regime [75]. This lifetime is enough for the charge transfer from the semiconductor to the specie adsorbed on the surface of the photocatalytic semiconductor [76]. Some factors help prevent electron–hole recombination. They are the incident light intensity and electronic structure of the semiconductor (Figure 4) [77]. When a photon with an energy equal to or greater than the band gap impacts a semiconductor, it promotes an electron to the CB, leaving a hole in the VB. The generated e- moves to the adsorbed organic species or solvent, due to which holes are generated on the exterior portion, i.e., the surface of the semiconductor. Electron transfer is duly facilitated by the substrate molecules on the catalyst surface [78]. In Figure 4, Path A shows the reduction of the electron-accepting species from the electron donated by the semiconductor surface. As evident from path B, due to the acceptance of the electron, a hole is also transferred to the semiconductor surface, which undergoes recombination with the electron from the donor species. The charge transfer rate via electron and hole depends on the band edge positions of VB and CB. Furthermore, the redox potential level is also crucial in determining the charge transfer rate. Electrons and holes can also undergo recombination in bulk semiconductors (Path D) or on the surface of semiconductors and cause a release of heat (Path C).

Heterogeneous photocatalysis involves the reaction in the adsorbed phase, as well as the entire process, which can be explained in the ensuing steps [72]:

i. The migration of reactants from the bulk of solutions to the photocatalyst's surface.
ii. Incorporation of the reactants from the exterior to the pore structures of the catalysts.
iii. At minimal, adsorption of one reactant shall occur.
iv. Response in the adsorbed stage.
v. The process of desorption of product.
vi. Product movement from the pore structure to the exterior.
vii. Movement of the products toward the bulk.

Photoexcitation in semiconductors is described in Figure 4.

## 7 Photocatalytic activity

The Beer–Lambert law governs photocatalytic activity. This law states "the absorption of a solution is directly proportional to the concentration of the compound" [79]

$$A = \varepsilon bc, \tag{1}$$

where $A$ is the absorbance and is a dimensionless term, $\varepsilon$ is the molar absorption coefficient (L $\text{mol}^{-1}$ $\text{cm}^{-1}$), $c$ is the concentration, where $b$ is the length of the cuvette in centimeters. The absorbance of the dye was found to be in direct relation to its concentration. The following expression determines photocatalytic degradation efficiency (PDE) [80]:

$$\%\text{PDE} = A_o - A_t/A_o \times 100, \tag{2}$$

where $A_o$ denotes the dye's initial absorbance, and $A_t$ indicates the dye's absorbance after time "*t*" is measured by ultraviolet–visible (UV–Vis) spectroscopy [81].

## 8 Choice of a photocatalyst

Semiconductors that absorb suitable energy light generate electron–hole pairs [82]. Thermodynamically, the VB of the semiconductor must have a higher oxidation potential than the oxidation potential of the dye molecules [77]. Similarly, for photo-reduction, the reduction potential of the CB must be more −ve than the chemical species' reduction potential. Regarding photocatalysis, the redox potential of the photo-generated VB hole shall be more positive than the water's oxidation potential to oxidize the water to yield hydroxyl ions [83]. Furthermore, the reduction–oxidation potential of the photo-generated electrons should be more −ve to reduce the "O" to superoxide anion. Semiconductors possessing low band gaps are ideal for photocatalytic degradation.

The following are some pre-requisites for an excellent semiconductor:

- Photoactive,
- Ability to utilize UV–Vis light,
- Photo-stable,
- Chemically and biologically inert, and
- Cost-effective.

Semiconductors, such as ZnS, CdS, CdSe, $TiO_2$, etc., are thoroughly investigated as suitable catalysts for the resourceful degradation of organic dyes.

## 9 General mechanism of semiconductor photocatalysis

During photocatalysis, the VB and CB of photocatalysts have active participation. The energy band gap ($E_g$) is the distance between the VB and CB. The light falling on the photocatalyst should have energy equal to or more than the energy of the band gap. When light falls on the photocatalyst, electrons in the VB become energized and migrate to the CB, leaving behind the positive hole. If recombining electron–hole pairs is avoided, they move toward the catalyst's surface, combining with adsorbed species [84]. The hydroxyl radical is formed when the hole combines with the water molecule. At the same time, electrons reduce oxygen to superoxide radicals. Hydroxyl radicals attack organic compounds to convert them to degradation products (water and carbon dioxide) [85]. Figure 5 shows the mechanism of photocatalysis.

The photocatalysis mechanism involves the following steps:

$$\text{Catalyst} + \text{hv} \rightarrow e^-_{cb} + h^+_{vb},$$

$$H_2O + h^+_{vb} \rightarrow OH^- + H^+,$$

$$O_2 + e^-_{cb} \rightarrow O^{-2},$$

$$O^{-2} + H^+ \rightarrow OH^{-2},$$

$$2OH^{-2} \rightarrow H_2O_2 + O_2,$$

$$H_2O_2 \rightarrow 2OH^{\cdot},$$

$$OH^{\cdot} + \text{Dye} \rightarrow CO_2 + H_2O.$$

## 10 Semiconductor as photocatalysts

Semiconductors are used as heterogeneous photocatalysts; they have filled VBs and vacant CBs [86,87]. The gap between these two bands is called a band gap which is larger in semiconductors than conductors (metals) and smaller in insulators (non-metals). Light energy excites the electron from the VB to the CB, leaving the hole behind.

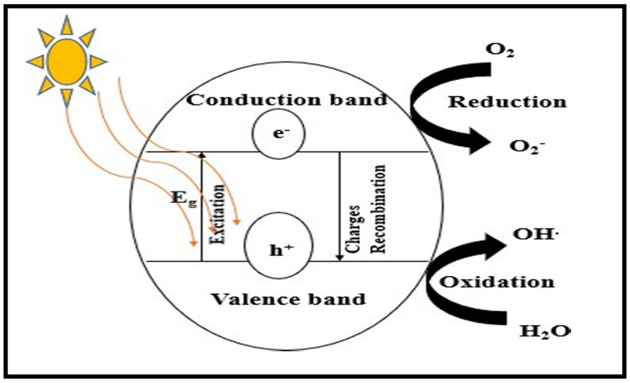

**Figure 5:** Mechanism of photocatalysis.

Photo-generated electron–hole pair is known as an exciton. Exciton has less life span, usually in nanoseconds. There are chances of an undesirable process, termed recombination, happening. Recombination is rejoining the photo-generated electron–hole pair and releasing energy as heat. Different factors are being manipulated to avoid recombination and make possible charge transfer to the adsorbed components, e.g., enhancing light intensity and structural changes in semiconductors. Structural features can be manipulated by decreasing the size of the photocatalyst up to the nanoscale. Nanowires, nanotubes, and nanoparticles are currently used for heterogeneous photocatalysis. Similarly, doping and nanocomposites are also promising in this regard. Semiconductors like ZnO [88,89], CdS [90,91], $TiO_2$ [92], ZnS [93], $ZrO_2$ [94], and $CeO_2$ [95–97] work as photocatalysts and mineralize organic pollutants into the less harmful state [98]. Every photocatalyst has a different band gap and requires wavelength of light according to the band gap. It could be calculated by using the following formula:

$$\lambda = \frac{1{,}240}{E_g}. \tag{3}$$

### 10.1 Visible light active photocatalyst

A visible light active photocatalyst is a material that can use visible light to promote a chemical reaction, usually in the presence of a catalyst, making them useful for many applications, including air and water purification and renewable energy production. Various metal oxides and sulfides are photoactive in visible light regions. Table 5 shows band gaps and certain other features of multiple semiconductors.

**Table 5:** Band gap ($E_g$) of semiconductor photocatalysts [99–115]

| Semiconductor | Band gap (eV) | Wavelength (nm) | Energy (kcal/mol) |
|---|---|---|---|
| $SnO_2$ | 3.8 | 326 | 87.7 |
| ZnO | 3.2 | 388 | 73.8 |
| ZnS | 3.6 | 344 | 83.1 |
| $WO_3$ | 3.2 | 388 | 73.8 |
| $TiO_2$ | 3.2 | 388 | 73.8 |
| $SrTiO_3$ | 3.2 | 388 | 73.8 |
| SiC | 3.0 | 413 | 69.2 |
| CdS | 2.5 | 496 | 57.5 |
| $Fe_2O_3$ | 2.3 | 539 | 53.1 |
| GaP | 2.25 | 551 | 51.9 |
| CdSe | 1.7 | 730 | 39.2 |
| $Bi_2O_3$ | 2.68 | 328 | 61.32 |

### 10.2 Features of efficient photocatalyst

According to the mechanism, light on a semiconductor generates electron–hole pairs [116]. The oxidation potential of the semiconductor VB should be more than the oxidation potential of organic compounds for charge carrier transfer, and the reduction potential of the CB should be lower than the reduction potential of chemical species. Regarding photocatalysis, the redox potential of the photo-generated VB hole shall be more +ve than the oxidation potential of water to oxidize the water to yield the OH. Furthermore, the redox potential of the photo-generated electrons must be more −ve to reduce the $O_2$ to superoxide anion ($O_2^-$). A promising photocatalyst should be photoactive, cost-effective, stable, inert, etc. [58].

## 11 Nanotechnology and nanomaterials

Nanotechnology is the science that deals with things at the nanoscale (1–100 nm). Materials having at least one dimension of nanoscale are termed nanomaterials. In 1959, physicist Richard Feynman seeded the concept of nanoscience in his talk, “There is Plenty of Room at the Bottom” by describing a synthesis process via manipulating atoms. This technology gained attention with the discovery of a scanning tunneling microscope in 1981. Later, fullerenes, carbon nanotubes, and metal oxide nanoparticles were discovered [117].

### 11.1 Nanostructures: classification by dimensions

Nanostructures are materials with at least one dimension in the 1–100 nm range. They can be classified based on their dimensions, and the most common classification is as follows:

1) **Zero-dimensional (0D) nanostructures** are nanoparticles or clusters with all dimensions in the nanoscale range. Examples include quantum dots, fullerenes, and metal clusters.
2) **One-dimensional (1D) nanostructures** have one dimension in the nanoscale range, and the other is much larger. Examples include nanowires, nanotubes, and nano-rods.
3) **Two-dimensional (2D) nanostructures** have two dimensions in the nanoscale range, and the third dimension is much larger. Examples include graphene, thin films, and nano-sheets.

4) **Three-dimensional (3D) nanostructures** are bulk materials with a nanoscale structure. The individual grains or domains in the material are nanoscale in size. Examples include nano-crystalline metals and ceramics [118,119].

The dimensionality of a nanostructure plays a vital role in its physical and chemical properties, and understanding these properties is essential for developing new applications in fields such as electronics, energy, and medicine.

## 11.2 Fabrication of nanostructures

Nanostructures can be synthesized by using two approaches.

### 11.2.1 Top-down approach

In this method, bulky materials are reduced in size to the nanometer range [120]. These nanostructures have some defects, like their surfaces are not smooth due to impurities leading to heat and electricity's low conductivity. Lithography, milling, aerosol spray, gas phase condensation, and atomic force manipulation come in this category. Nanostructures made by this approach find applications in different fields.

### 11.2.2 Bottom-up approach

This approach is based on fabricating nanostructures from smaller units to combine and make larger units (nanoscale) [120]. It is also called self-assembly. It is inspired by natural biological systems, where essential structures are constructed by chemical forces joining the smaller units. Self-assembled nanostructures have comparatively fewer defects (Figure 6). Different fabrication methods like sol–gel, microwave synthesis, colloidal dispersion methods, vapor phase deposition methods, hydrothermal methods, and combustion processes are included in this approach [121].

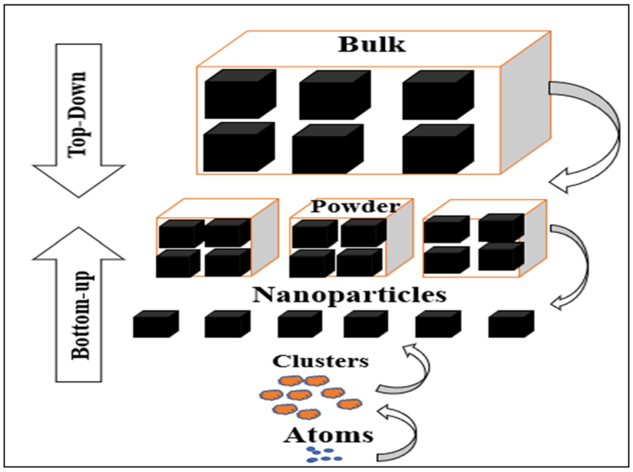

**Figure 6:** Top-down and bottom-up approach to fabrication of nanostructures.

Metal oxide nanoparticles and nanocomposites offer several advantages and disadvantages regarding their physicochemical properties. One benefit is their high surface area-to-volume ratio, which increases reactivity and facilitates efficient catalytic reactions [122]. Furthermore, their compact size enables excellent dispersion and accessibility to target pollutants [123]. Tunable features of metal oxide nanoparticles and nanocomposites, such as band gap and shape, may also be adjusted for specific applications. Furthermore, because of their distinct physicochemical characteristics, they display improved photocatalytic activity, making them excellent candidates for water treatment. However, there are several drawbacks to using these nanomaterials. Agglomeration and aggregation are significant issues that contribute to diminished responsiveness and efficiency.

Additionally, the possibility of metal ion leakage from nanomaterials raises worries about their long-term environmental impact. Furthermore, producing and characterizing metal oxide nanoparticles and nanocomposites can be complicated, necessitating careful control over experimental conditions. While metal oxide nanoparticles and nanocomposites offer numerous advantages regarding their physicochemical properties, carefully considering their limitations and potential risks is necessary for their safe and effective implementation [124].

## 12 Photocatalysts at nanoscale

Semiconductors at the nanometer scale have a lot of differences from bulk. With the reduction of size, large surface area, electrical and optical properties are being manipulated. The color of nanoparticles and bulk semiconductors is not the same; e.g., gold nanoparticles have a red color [125]. The quantum confinement effect becomes pronounced when the size is reduced to the Bohr radius of the first excitation or becomes equal to the electron's wavelength [126]. Quantum confinement restricts the random motion of free electrons to quantized energy levels. These quantized energy levels are discrete energy states having fixed energy, resulting in a wide band gap. Semiconductors with particle size reduction lead to blue shift and move toward shorter wavelengths [127]. It happens due to a larger band gap; energy levels of VB slightly move toward low energies while CB vigorously moves to higher ones. At the nanoscale, the surface area is increased, resulting in higher photocatalytic degradation of dyes [71,128–130]. A high surface-to-volume ratio enhances the surface phenomena [131]. That is why semiconductor nanoparticles have been extensively used as photocatalyst for dye degradation.

## 12.1 Kinetic model of semiconductor photocatalysis

The Langmuir–Hinshelwood model presents a kinetic analysis of photocatalysis [132]. According to the law of mass action, photocatalytic degradation of dye follows a quasi-first-order reaction. So, the rate is

$$r = -\mathrm{d}C(t)/\mathrm{d}t = k_{\mathrm{obs}}C(t), \tag{4}$$

where $k_{\mathrm{obs}}$ is the rate constant, and $C(t)$ is the concentration of dye, which is adsorbed on the surface of semiconductors at time $t$. For dye photo-degradation, adsorption–desorption (A–D) is mandatory, which follows the Langmuir adsorption isotherm. If A–D equilibrium is maintained, then the above equation becomes

$$r = k_{\mathrm{obs}}KC/1 + KC, \tag{5}$$

where $K$ is the A–D equilibrium constant, $C$ is the reactive concentration of solution at time $t$, and $KC$ is less than one as in photocatalytic reaction concentration of dye is less, so equation (5) would become

$$r = -\mathrm{d}C(t)/\mathrm{d}t = k_{\mathrm{obs}}KC = kC, \tag{6}$$

where $k$ is the apparent rate constant and is equal to the product of $k_{\mathrm{obs}}$ and $K$, and the following equation is obtained by integrating the above equation within limits 0–1:

$$\mathrm{In}C_{\mathrm{o}}/C_{\mathrm{t}} = kt, \tag{7}$$

where $C_{\mathrm{o}}$ is the initial concentration before illumination and $C_{\mathrm{t}}$ is the concentration at illumination time $t$ [133]. The half-life for such reactions is analogous to the half-life of first-order reaction.

$$t_{1/2} = \frac{0.693}{k}, \tag{8}$$

where $t_{1/2}$ is the half-life having a unit (min).

# 13 Photo-degradation by metal oxide

Photocatalysis is a safe, long-lasting, and ecologically benign method of decomposing or degrading organic contaminants. Since the dangerous molecules are destroyed or changed into nontoxic forms, photocatalytic remediation technology eliminates organic pollutants from contaminated water without leaving toxic leftovers. A complicated oxidative process called photocatalytic remediation occurs when a photocatalyst is present. Energy levels that are equivalent to or higher than the band gap energy between the VB and CB of the photocatalyst are absorbed by photocatalytic materials. Exciting electrons from the VB to the CB with photon absorption results in charge separation, which creates positive holes in the VB [134]. Positive holes either oxidized water to produce hydroxyl radicals ($OH^{\bullet}$) or impurities in the CB, while excited electrons reduce the oxygen absorbed by the photocatalyst. The organic pollutants are attacked by the $OH^{\bullet}$ free radical, which undergoes a series of reactions to completely decompose them into $CO_2$ and $H_2O$ or transform them into nontoxic and non-hazardous forms.

On the contrary, the photo-generated electron and hole pairs have a strong recombination propensity, reducing photocatalysis's efficiency. The recombination of photo-generated charge carriers must be minimized or managed to allow photocatalytic reactions. The type and nature of photocatalysts, organic pollutants, the reaction medium's pH and temperature, the reaction medium's light source and intensity, the presence of the solvent and sacrificial reagents, and other factors all affect how effectively organic pollutants are degraded by photocatalysis for wastewater remediation. The organic pollutants' chemical composition and associated functional groups also impacted the photocatalytic reactions.

The photocatalytic degradation of dangerous and toxic organic pollutants into nontoxic and gaseous chemicals has been studied using a wide range of metal oxide/semiconductor-based nanomaterials. As discussed in this section, using metal oxide nanoparticles for photocatalytic degradation of organic contaminants in water remediation applications is advancing.

Hosseini and Saeedi have studied the photo-degradation of Rhodamine B by bismuth oxide ($Bi_2O_3$) NPs, synthesized by the chemical precipitation method. NPs were well crystallized, and the crystal size was 22.4 nm by characterizing the sample via X-ray diffraction (XRD), scanning electron microscopy (SEM), and Fourier transform infrared (FT-IR). Under optimal conditions, i.e., at a catalyst dosage of 12.5 mg/L for 2 h at pH 7, 95% of the dye was degraded [135]. An orthorhombic phase of tin sulfide nanoparticles was synthesized through a sonochemical method at a different frequency and used for photo-degradation of methyl blue dye and concluded that the photocatalytic activity of SnS nanoparticles synthesized at a lower sonication frequency was higher. About 50% of the methyl blue dye was degraded in just 45 min at low frequency, and at high frequency, it took 60 min to degrade 50% of the dye [136]. Chen et al. studied the photo-degradation of MG dye by $TiO_2$ NPs. The solution containing 0.50 g/L dye and 0.5 g/L $TiO_2$ was irradiated for 4 h and degraded 99.9%. The results show that the dye's chromophoric structure cleaves stepwise by forming five different intermediates during the degradation. These intermediates were confirmed by the high-performance liquid chromatography–photodiode array–electrospray ionization mass spectrometry technique [137]. Alinsafi et al. employed titania $TiO_2$ to degrade industrial dyes like reactive azoic and metal phthalocyanines under solar and UV irradiation. PDE came out to be 74%. They observed that titania was also effective for wastewater with a higher pH value [84]. Qutub et al. synthesized cadmium sulfide nanoparticles (CdS NPs) using different precursors as sulfide sources. The photocatalytic efficiency of the synthesized photocatalysts was studied by degrading acid blue 29 dye under visible light. The enhanced photocatalytic activity was attributed to a reduction in size [138]. Chandran et al. synthesized CdS NPs, and their size was found to be 18 nm, and their shape was spherical. The particles were more stable after 30 days of incubation in a static environment. The degradation of methylene blue (MB) dye under solar irradiation was used to test the photocatalytic activity of CdS NPs. At pH 8, the highest photo-activity was recorded [139]. Jan et al. studied the photocatalytic degradation of acid violet 17 dye by Sr-doped ZnO nanoparticles. They used UV–Vis, XRD, SEM, FT-IR, and energy dispersive X-ray (EDX) to characterize synthesized nanoparticles. The particle size was calculated to be 16 and 21 for ZnO and Sr-ZnO, respectively. The photocatalytic activity is increased with increasing pH of the medium. Almost 88% of the dye was degraded in 140 min of irradiation and using a ZnO photocatalyst [140]. Table 6 displays the photocatalytic degradation of organic dyes by metal oxide.

## 14 Photo-degradation by nanocomposites

Zeng et al. used nickel/nickel oxide-cellulose filter paper composite (Ni@FP) to degrade methyl orange. The *in situ* reduction reaction under average temperature and pressure prepared these materials. SEM, X-ray photoelectron spectroscopy (XPS), FT-IR, and XRD characterized the synthesized materials. In this article, they found the PDE of the synthesized Ni@FP material to be 93.40% in just 5 min at pH 8 [141].

Under UV light illumination, Hunge et al. examined the photocatalytic activity of $TiO_2$@nanodiamond composites. When the 10 ppm solution of bisphenol A was exposed under UV irradiation, the $TiO_2$@nanodiamond photocatalyst destroyed bisphenol A completely in 100 min [142].

Mohamed et al. investigated malachite green (MG) for photocatalytic degradation by polyacrylonitrile (PAN) nanofiber/biogenic silica composite nanofibers. This photocatalyst was made using PAN nanofibers that were electrospun and then cross-linked with diatomite and rice husk nano-silica, two types of biogenic silica. SEM, transmission electronic microscopy (TEM), EDX, FT-IR, and XRD techniques were used to characterize the produced materials.

A significant factor that affects photo-degradation effectiveness is pH. The mean pH of the reaction medium significantly influences the surface characteristics of the two biogenic silica membranes. Setting the medium neutral resulted in the most significant photocatalytic degradation, which was reduced by 98% in less than 10 min. Low photo-degradation efficiency is caused by the rivalry between hydrogen ions and MG cations for active sites on the surface of adsorbents in an acidic medium (pH 4). This competition reduced the number of active sites accessible to bind MG cations. The positive charge density on membrane surface sites decreases as the pH rises, which increases the prepared membranes' capacity to bind MG. The hydroxyl groups of silica remain negatively charged under neutral conditions (pH 7), despite the entire

**Table 6:** Photocatalytic degradation of organic dyes by metal oxide

| Sr. No | Photocatalyst | Pollutant organic dye | Time of irradiation | pH | %PDE | References |
|---|---|---|---|---|---|---|
| 1 | $Bi_2O_3$ | Rhodamine B | 2 h | 7 | 95 | [135] |
| 2 | Tin sulfide | Methyl blue | 1 h | | 50 | [136] |
| 3 | $TiO_2$ | MG | 4 h | | 99.9 | [137] |
| 4 | $TiO_2$ | Azoic and metal phthalocyanines | 5 h | 11 | 74 | [36] |
| 5 | Cadmium sulfide | Acid blue 29 | 1.5 h | — | 79 | [138] |
| 6 | Cadmium sulfide | Methyl blue | 1 h | 8 | 88 | [139] |
| 7 | ZnO | Acid violet 17 | 2 h and 20 min | 9 | 88 | [140] |

membrane being positively charged. MG was more readily adsorbable due to the electrostatic affinity between the positively charged hydroxyl groups and the negatively charged MG ions [143].

The type and nature of photocatalysts, organic pollutants, the reaction medium's pH and temperature, the reaction medium's light source and intensity, the presence of the solvent and sacrificial reagents, and other factors all affect how effectively organic pollutants are degraded by photocatalysis for wastewater remediation. The organic pollutants' chemical composition and associated functional groups also impacted the photocatalytic reactions. The photocatalytic degradation of dangerous and toxic organic pollutants into nontoxic and gaseous chemicals has been studied using a wide range of metal oxide/semiconductor-based nanomaterials. As discussed in this section, using metal oxide nanoparticles for the photocatalytic degradation of organic contaminants in water remediation applications is advancing. The pH of the dye solution affects how photocatalysis functions. Mainly, pH is essential for the degradability of anionic and cationic dyes. Anionic dye is often degraded by acidic pH, while cationic dye is demonstrated to be degraded by basic pH. In this study, they looked at the relative degradability of cationic and anionic dye while keeping the pH of the solution at 7.2. Compared to pristine $TiO_2$ at pH 7.2, the graphene–$TiO_2$ composite showed a 15- and 3.5-fold increase in Congo red and MB dye degradability, respectively. They studied its photocatalytic activity under natural sunlight and UV-filtered sunlight irradiation. They highlight the superior efficacy of the visible portion of the solar spectrum in harvesting composite deterioration and the insignificant impact of the UV band of sunlight [144].

Titanium dioxide nano-particles@nitrogen-doped carbon nanocomposite ($TiO_2$ NPs@C) was the subject of research by Atchudan et al. The catalysts were made using a low-cost hydrothermal process, and attenuated total reflectance was used to examine their physical and chemical characteristics by field emission SEM, XRD, XPS, ATR-FTIR spectroscopy, EDX, and elemental mapping analysis. We looked into the photocatalytic efficiency of a produced $TiO_2$ NPs@C nanocomposite in the breakdown of MB when exposed to UV light. The degrading efficiency of the created $TiO_2$ NPs@C nanocomposite is more significant when compared to bare $TiO_2$ NPs. The degradation efficiency of the synthesized $TiO_2$ NPs@C nanocomposite is over 90% when the irradiation period is extended to 40 min, which is much higher than the degradation efficiency of the bare $TiO_2$ NPs, about 39%. The improved photocatalytic activity of the $TiO_2$ NPs@C nanocomposite was due to the synergistic effect of $TiO_2$ NPs and graphene-like carbon. Moreover, carbon obtained from a green, natural source has oxygen- and nitrogen-containing groups on its surface, leading to more hydroxyl and superoxide radicals and effective photocatalytic activity [145].

Using hybrid diatomite/ZnFe layered double hydroxide composites, Zhao et al. examined the degradation of MB and MG under visible light irradiation (DZF). It was simple to create the composites utilizing the co-precipitation approach. In 180 and 150 min, the DZF degraded 94.46% of MB and 97.02% of MG, respectively. Due to the synergistic effects of the quick charge separation rates brought on by the creation of heterostructures between diatomite and pure ZnFe-LDH, strong visible light absorption, wide surface area, and pore volume, the hybrid nanocomposite DZF has a more excellent photo-degradation activity than ZF [146]. Recently, Liu et al. [148], Chen et al. [149], and He et al. [150] examined the treatment of CrVI-containing $Mg(OH)_2$ nanowaste, photocatalytic performance of S-scheme $CdMoO_4$/CdO nanosphere, and generation of acyl radicals from form-amides and aldehydes, respectively. Mechanism of electrostatic potential changes regulated via adsorption speciation and combination of catalysis and fluorescence toward the detection of $H_2O_2$ and 2,4-DNP and fluorophore molecule loaded in Tb-MOF for dual-channel fluorescence chemo-sensor applications are explored by Ma et al. [151] and Li et al. [152,153]. Some other recent developments in chemical neutral organic compounds,

**Table 7:** Photocatalytic degradation of organic dyes by nanocomposites

| Sr. No | Photocatalyst | Pollutant organic dye | Time of irradiation (min) | pH | %PDE | Reference |
|---|---|---|---|---|---|---|
| 1 | Ni@FP | Methyl orange | 5 | 8 | 93.40 | [141] |
| 2 | $TiO_2$@nanodiamond | Bisphenol A | 100 | 5.1 | 100 | [142] |
| 3 | PAN/biogenic silica | MG | 10 | 7 | 98 | [143] |
| 4 | G-$TiO_2$ | Congo red and MB | 60 | 7.2 | 90 | [144] |
| 5 | $TiO_2$ NPs@C | MB | 40 | _ | 90 | [145] |
| 6 | DZF | MB and MG | 180 min<br>150 min | _ | 94.46,<br>97.02 | [146] |
| 7 | $ZnFe_2O_4$/ZnO | MB and RBB | 120 | 11 | 80 | [147] |

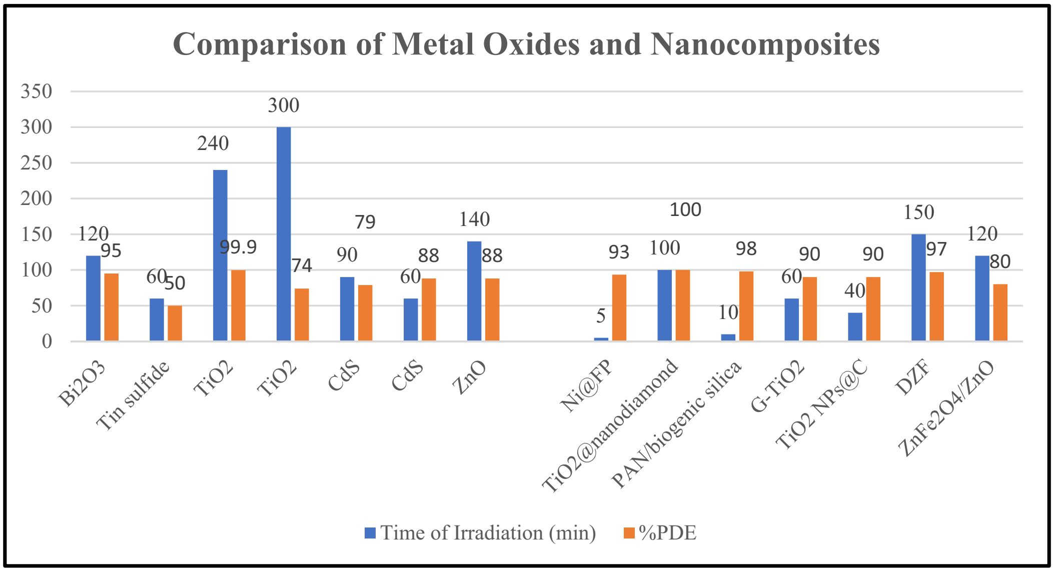

**Figure 7:** Comparison of the %PDE by metal oxide and nanocomposite.

metal–organic systems, and photocatalytic degradation of refractory contaminants are reported by Chen et al. [154], Li et al. [155], and Zheng et al. [156]. Wang et al. [157] and Kong et al. [158] highlight the performance of *Alcaligenes* sp. TB by Pd stimulating to produce membrane adaptation mechanism and enhanced red luminescence in CaAl12O19:Mn4$^{+}$ via doping Ga3$^{+}$ for plant growth lighting, respectively.

A composite catalyst made of $ZnFe_2O_4$ and ZnO was produced by Zouhier et al. using the solution combustion method. The manufactured catalysts were examined using XRD, XPS, X-ray fluorescence, SEM, TEM, and UV–Vis diffuse spectroscopy. The degradation of two dyes, MB and Remazol Brilliant Blue (RBB), in an aqueous solution under both UV and visible light illumination, was used to test the photocatalytic activities of the catalysts. It was found that the composite showed good photocatalytic activity at basic pH for both MB and RBB using one g/L of the catalyst under UV light. The combination demonstrated exceptional visual efficiency, reaching an 80% conversion of the initial dye concentrations in 2 h, whereas virgin ZnO had no activity under visible illumination. The creation of $ZnFe_2O_4$ associated with ZnO, which has a narrow band gap and contributes to visible photon absorption with an improved separation path for the photo-generated carriers, is thought to be the cause of the Fe/ZnO sample's increased visible photocatalytic activity over pure ZnO (Table 7).

This study investigated various parameters for dye photodegradation, including catalyst dosage, initial dye concentrations, and solution pH. They concluded that increasing the catalyst amount and initial dye concentrations increased the photodegradation efficiency of the catalyst up to a certain point before decreasing. The following is an explanation for these phenomena:

1) When photocatalyst mass increases, more active catalyst surface sites are available. The levels of hydroxyl and superoxide radicals therefore rise. The dye degradation efficiency decreases as the catalyst mass expands because the turbidity of the solution makes it harder for light to penetrate and activate the entire catalyst suspension.
2) The likelihood of contact between the dye molecules and the oxidant species, which would increase the degradation rate, rises as the initial concentrations of the dyes do as well. Unfortunately, when dye concentrations are too high at first, solutions become opaque, which means that photons that must interact with the catalyst surface are caught and absorbed by the dye solution, restricting photon absorption by the catalyst and lowering decolorization efficiency [147].

## 15 Comparative analysis of the data

Metal oxides and nanocomposites both show photo-degradation efficiency under solar irradiation. But from the comparative analysis in Figure 7, nanocomposites show the best performance compared to metal oxides. Nanocomposites degrade the toxic organic dye in less time, while it takes more time to degrade pollutant organic dye than metal oxide. Besides time duration, the degradation efficiency of the nanocomposites is also high. Nanocomposites degrade almost all toxic dyes, while the percent photodegradation efficiency of the metal oxide is below 90%.

In metal oxide, the best performers are the bismuth oxide and titania. $Bi_2O_3$ degraded 95% of the organic dye in 120 min and functionalized $TiO_2$ degraded 99.9% toxic dye in 240 min. ZnO and CdS are promising photocatalysts as compared to SnS. Tin sulfide is the worst performer among all these photocatalysts, which degrade only 50% in 60 min. In the case of nanocomposites, the best performer is Ni@FP. Nickel/nickel oxide-cellulose filter paper composite degrades 93% methyl orange in just 5 min of solar irradiation, and it is such quick and immediate photo-degradation of the dye by the nanocomposite. $TiO_2$@nanodiamond is also a promising photocatalyst, which degrades the organic dye completely in 100 min. Overall, nanocomposites efficiently degrade toxic organic dye.

## 16 Future perspective of the study

The world is going to industrialize more and more in the future. As a result of its changes, water is getting more and more polluted. So, there is a dire need for wastewater treatment. In this regard, photocatalysis is one of the best nanotechnology wastewater treatments, which treats pollutants and plays a role in wastewater treatment. As mentioned in the above section, nanocomposites are the best photocatalyst compared to metal oxide nanoparticles. In the group of metal oxide, $Bi_2O_3$ and $TiO_2$ show more PDE among all. So, in future studies, we can synthesize the nanocomposite of $Bi_2O_3$@ $TiO_2$. By synthesizing the composite of $Bi_2O_3$@ $TiO_2$, we can predict that it will show the best photocatalytic activity. Besides this, if the synthesized nanocomposite is doped with Nickel atoms, it will show even better results, as the Ni@FP %PDE predicted. So, in future research work, the Ni–$Bi_2O_3$@ $TiO_2$ will be synthesized for the photo-degradation of organic dye and wastewater treatment.

## 17 Conclusion

The comprehensive review of metal oxides and nanocomposites for the photocatalytic degradation of organic dyes highlights their significant role in mitigating water pollution resulting from industrial waste. The comparative analysis of metal oxides and nanocomposites for photocatalytic degradation of organic dyes reveals a significant efficiency advantage in favor of nanocomposites. The data indicate that nanocomposites not only achieve a high %PDE but also require considerably less time to do so. For instance, the Ni@FP stands out with an impressive %PDE of 93 achieved in a mere 5 min of irradiation, showcasing its potential for rapid and effective wastewater treatment $TiO_2$@nanodiamond composite achieves complete degradation with a %PDE of 100 within 100 min. These findings suggest that incorporating nanocomposites, particularly those like Ni@FP and $TiO_2$@nanodiamond, could significantly enhance the efficiency and practicality of photocatalytic processes in water treatment applications. The metal oxides, while effective, exhibit lower %PDEs and longer irradiation times, with $Bi_2O_3$ and two forms of $TiO_2$ showing varied efficiencies under different conditions. Overall, the trend indicates a promising future for nanocomposite applications in environmental remediation strategies, especially in industrialized settings where rapid and efficient water purification is paramount. Innovations in semiconductor photocatalysis, particularly at the nanoscale, have revealed promising approaches to enhance the degradation rates of toxic dyes, contributing to more effective and sustainable water purification methods. The advancements in the synthesis and characterization of photocatalysts, including the exploration of doping and the creation of hybrid structures, offer a pathway to optimize the photo-degradation process further. The insights provided by this review pave the way for future research focused on developing more efficient and cost-effective photocatalysts. The potential for industrial application of these findings could significantly impact environmental remediation efforts, contributing to the provision of cleaner water resources and the overall improvement of ecosystem health.

**Acknowledgments:** Researchers Supporting Project number (RSPD2024R576), King Saud University, Riyadh, Saudi Arabia.

**Funding information:** The research is financially supported by Researchers Supporting Project number (RSPD2024R576), King Saud University, Riyadh, Saudi Arabia.

**Author contributions:** Yousaf Khan, Fuad A. Awwad: conceptualization, writing – original draft, methodology, investigation, formal analysis, data curation; Muhammad Naeem Khan: conceptualization, writing – original draft, visualization, software, formal analysis, data curation; Abdul Salam: methodology, formal analysis, data curation; Haleema Sadia: writing – review and editing, visualization, software, formal analysis; Muhammad Farhat Ullah, Emad A. A. Ismail: writing – review and editing, methodology; Barno Sayfutdinovna Abdullaeva: writing – review and editing, data curation; Muhammad Ijaz Khan: Supervision, formal analysis.

**Conflict of interest:** The authors declare that they have no competing interests.

**Ethical approval:** The conducted research is not related to either human or animal use.

**Data availability statement:** The data sets generated during and/or analyzed during the current study are available from the corresponding author upon reasonable request.

# References

[1] Ameen S, Murtaza M, Arshad M, Alhodaib A, Waseem A. Perovskite $LaNiO_3/Ag_3PO_4$ heterojunction photocatalyst for the degradation of dyes. Front Chem. 2022;10:969698.

[2] Mokarram M, Saber A, Sheykhi V. Effects of heavy metal contamination on river water quality due to release of industrial effluents. J Clean Prod. 2020;277:123380.

[3] Rafiq A, Ikram M, Ali S, Niaz F, Khan M, Khan Q, et al. Photocatalytic degradation of dyes using semiconductor photocatalysts to clean industrial water pollution. J Ind Eng Chem. 2021;97:111–28.

[4] Liu L, Chen Z, Zhang J, Shan D, Wu Y, Bai L, et al. Treatment of industrial dye wastewater and pharmaceutical residue wastewater by advanced oxidation processes and its combination with nanocatalysts: A review. J Water Process Eng. 2021;42:102122.

[5] Varjani S, Joshi R, Srivastava VK, Ngo HH, Guo W. Treatment of wastewater from petroleum industry: current practices and perspectives. Environ Sci Pollut Res. 2020;27(22):27172–80.

[6] Ademe AS, Alemayehu M. Source and determinants of water pollution in Ethiopia: Distributed lag modeling approach. Intellect Prop Rights: Open Access. 2014;2:1000110.

[7] Singh N, Nagpal G, Agrawal S. Water purification by using adsorbents: a review. Environ Technol Innov. 2018;11:187–240.

[8] Reza MS, Yun CS, Afroze S, Radenahmad N, Bakar MSA, Saidur R, et al. Preparation of activated carbon from biomass and its applications in water and gas purification, a review. Arab J Basic Appl Sci. 2020;27(1):208–38.

[9] Palaniappan M, Gleick PH, Allen L, Cohen MJ, Christian-Smith J, Smith C, et al. Clearing the waters: a focus on water quality solutions. UNEP. Nairobi: Pacific Institute; 2010.

[10] Rayaroth MP, Aravindakumar CT, Shah NS, Boczkaj G. Advanced oxidation processes (AOPs) based wastewater treatment-unexpected nitration side reactions-a serious environmental issue: A review. Chem Eng J. 2022;430:133002.

[11] Oturan MA, Aaron J-J. Advanced oxidation processes in water/wastewater treatment: principles and applications. A review. Crit Rev Environ Sci Technol. 2014;44(23):2577–641.

[12] Luo M, Zhou H, Zhou P, Lai L, Liu W, Ao Z, et al. Insights into the role of in-situ and ex-situ hydrogen peroxide for enhanced ferrate (VI) towards oxidation of organic contaminants. Water Res. 2021;203:117548.

[13] Sacco O, Vaiano V, Daniel C, Navarra W, Venditto V. Highly robust and selective system for water pollutants removal: How to transform a traditional photocatalyst into a highly robust and selective system for water pollutants removal. Nanomaterials. 2019;9(11):1509.

[14] Lee S, Bae H-S, Choi W. Selective control and characteristics of water oxidation and dioxygen reduction in environmental photo (electro) catalytic systems. Acc Chem Res. 2023;56(7):867–77.

[15] Noor S, Ashar A, Taj MB, Bhutta ZA. Advanced oxidation processes for remediation of persistent organic pollutants. Advanced oxidation processes for wastewater treatment. Taylor & Francis group; 2022. p. 203–12.

[16] Gürses A, Açıkyıldız M, Güneş K, Gürses MS. Classification of dye and pigments. Dyes and pigments. Springer; 2016. p. 31–45.

[17] Gusain R, Gupta K, Joshi P, Khatri OP. Adsorptive removal and photocatalytic degradation of organic pollutants using metal oxides and their composites: A comprehensive review. Adv Colloid Interface Sci. 2019;272:102009.

[18] Gürses A, Açıkyıldız M, Güneş K, Gürses MS. Dyes and pigments: their structure and properties. Dyes and Pigments. Germany: Springer; 2016. p. 13–29.

[19] Zollinger H. Color chemistry: syntheses, properties, and applications of organic dyes and pigments. John Wiley & Sons; 2003.

[20] Kumar A, Dixit U, Singh K, Gupta SP, Beg MSJ. Structure and properties of dyes and pigments. Dye Pigments-Novel Appl Waste Treat. IntechOpen; 2021.

[21] Shindy H. Basics in colors, dyes and pigments chemistry: A review. Chem Int. 2016;2(29).

[22] El Harfi S, El Harfi A. Classifications, properties and applications of textile dyes: A review. Appl J Environ Eng Sci. 2017;3(3):00000-3, 311–20.

[23] Ozdemir O, Armagan B, Turan M, Celik MS. Comparison of the adsorption characteristics of azo-reactive dyes on mezoporous minerals. Dye Pigment. 2004;62(1):49–60.

[24] Benkhaya S, M'rabet S, El Harfi A. A review on classifications, recent synthesis and applications of textile dyes. Inorg Chem Commun. 2020;115:107891.

[25] Benkhaya S, M'rabet S, El Harfi A. Classifications, properties, recent synthesis and applications of azo dyes. Heliyon. 2020;6(1):e03271.

[26] Hicham Z, Bencheqroun Z, El Mrabet I, Neves I. Removal of basic dyes from aqueous solutions by adsorption onto Moroccan clay (Fez city). Mediterr J Chem. 2019;8(3):158–67.

[27] Shabir M, Yasin M, Hussain M, Shafiq I, Akhter P, Nizami A-S, et al. A review on recent advances in the treatment of dye-polluted wastewater. J Ind Eng Chem. 2022;112:1–19.

[28] Klimaviciute R, Riauka A, Zemaitaitis A. The binding of anionic dyes by cross-linked cationic starches. J Polym Res. 2007;14:67–73.

[29] Cestari AR, Vieira EF, Dos Santos AG, Mota JA, De Almeida VP. Adsorption of anionic dyes on chitosan beads. 1. The influence of the chemical structures of dyes and temperature on the adsorption kinetics. J Colloid Interface Sci. 2004;280(2):380–6.

[30] Affat SS. Classifications, advantages, disadvantages, toxicity effects of natural and synthetic dyes: a review. Univ Thi-Qar J Sci. 2021;8(1):130–5.

[31] Attallah OA, Al-Ghobashy MA, Nebsen M, Salem MY. Removal of cationic and anionic dyes from aqueous solution with magnetite/pectin and magnetite/silica/pectin hybrid nanocomposites: kinetic, isotherm and mechanism analysis. RSC Adv. 2016;6(14):11461–80.

[32] Atas MS, Dursun S, Akyildiz H, Citir M, Yavuz CT, Yavuz MS. Selective removal of cationic micro-pollutants using disulfide-linked network structures. RSC Adv. 2017;7(42):25969–77.

[33] Chiou M-S, Ho P-Y, Li H-Y. Adsorption of anionic dyes in acid solutions using chemically cross-linked chitosan beads. Dye Pigment. 2004;60(1):69–84.

[34] Iram M, Guo C, Guan Y, Ishfaq A, Liu H. Adsorption and magnetic removal of neutral red dye from aqueous solution using Fe3O4 hollow nanospheres. J Hazard Mater. 2010;181(1–3):1039–50.

[35] Hassan QM, Emshary C, Sultan H. Investigating the optical non-linear properties and limiting optical of eosin methylene blue solution using a cw laser beam. Phys Scr. 2021;96(9):095503.

[36] Barcia JJ. The Giemsa stain: its history and applications. Int J Surg Pathol. 2007;15(3):292–6.

[37] Hong JY, Park NH, Yoo KH, Hong J. Comprehensive impurity profiling and quantification of Sudan III dyes by gas chromatography/mass spectrometry. J Chromatogr A. 2013;1297:186–95.

[38] Rekha R, Ramalingam A. Nonlinear characteristic and optical limiting effect of oil red O azo dye in liquid and solid media. J Mod Opt. 2009;56(9):1096–102.

[39] Maurya N, Mittal A. Biosorptive uptake of cationic dyes from aqueous phase using immobilised dead macro fungal biomass. Int J Environ Technol Manag. 2011;14(1–4):282–93.

[40] Choi I-H, Bin Yoon S, Huh S, Kim S-J, Kim Y. Photophysical properties of cationic dyes captured in the mesoscale channels of micron-sized metal-organic framework crystals. Sci Rep. 2018;8(1):1–12.

[41] Ramalingam G, Nagapandiselvi P, Priya A, Rajendran S. A review of graphene-based semiconductors for photocatalytic degradation of pollutants in wastewater. Chemosphere. 2022;300:134391.

[42] Daneshvar N, Salari D, Khataee A. Photocatalytic degradation of azo dye acid red 14 in water on ZnO as an alternative catalyst to $TiO_2$. J Photochem Photobiol A: Chem. 2004;162(2–3):317–22.

[43] Altun EY, Şişmanoğlu ZT, Soylu GSP. Photocatalytic decomposition of textile dyestuffs by photosensitive metal oxide catalysts. Turkish J Chem. 2021;45(5):1432–43.

[44] Donkadokula NY, Kola AK, Naz I, Saroj D. A review on advanced physico-chemical and biological textile dye wastewater treatment techniques. Rev Environ Sci bio/technology. 2020;19:543–60.

[45] Aldalbahi A, El-Naggar ME, El-Newehy MH, Rahaman M, Hatshan MR, Khattab TA. Effects of technical textiles and synthetic nanofibers on environmental pollution. Polymers. 2021;13(1):155.

[46] Bhattacharjee R, Mitra T, Mitra P, Biswas S, Ghosh S, Chattopadhyay S et al. Effective materials in the photocatalytic treatment of dyestuffs and stained wastewater. Trends and Contemporary Technologies for Photocatalytic Degradation of Dyes. Germany: Springer; 2022. p. 173–200.

[47] Nagarajan D, Kusmayadi A, Yen H-W, Dong C-D, Lee D-J, Chang J-S. Current advances in biological swine wastewater treatment using microalgae-based processes. Bioresour Technol. 2019;289:121718.

[48] Crini G, Lichtfouse E. Advantages and disadvantages of techniques used for wastewater treatment. Env Chem Lett. 2019;17:145–55.

[49] Ahmed S, Mofijur M, Nuzhat S, Chowdhury AT, Rafa N, Uddin MA, et al. Recent developments in physical, biological, chemical, and hybrid treatment techniques for removing emerging contaminants from wastewater. J Hazard Mater. 2021;416:125912.

[50] Ma D, Yi H, Lai C, Liu X, Huo X, An Z, et al. Critical review of advanced oxidation processes in organic wastewater treatment. Chemosphere. 2021;275:130104.

[51] Garrido-Cardenas JA, Esteban-García B, Agüera A, Sánchez-Pérez JA, Manzano-Agugliaro F. Wastewater treatment by advanced oxidation process and their worldwide research trends. Int J Environ Res Public Health. 2020;17(1):170.

[52] Carolin CF, Kumar PS, Joshiba GJ. Sustainable approach to decolourize methyl orange dye from aqueous solution using novel bacterial strain and its metabolites characterization. Clean Technol Environ Policy. 2021;23:173–81.

[53] Varjani S, Rakholiya P, Ng HY, You S, Teixeira JA. Microbial degradation of dyes: an overview. Bioresour Technol. 2020;314:123728.

[54] Bal G, Thakur A. Distinct approaches of removal of dyes from wastewater: A review. Mater Today: Proc. 2022;50:1575–9.

[55] Selvaraj V, Karthika TS, Mansiya C, Alagar M. An over review on recently developed techniques, mechanisms and intermediate involved in the advanced azo dye degradation for industrial applications. J Mol Struct. 2021;1224:129195.

[56] Boochakiat S, Inceesungvorn B, Nattestad A, Chen J. Bismuth–based oxide photocatalysts for selective oxidation transformations of organic compounds. ChemNanoMat. 2023;9(7):e202300140.

[57] Dong S, Cui L, Zhang W, Xia L, Zhou S, Russell CK, et al. Double-shelled $ZnSnO_3$ hollow cubes for efficient photocatalytic degradation of antibiotic wastewater. Chem Eng J. 2020;384:123279.

[58] Chen D, Cheng Y, Zhou N, Chen P, Wang Y, Li K, et al. Photocatalytic degradation of organic pollutants using $TiO_2$-based photocatalysts: A review. J Clean Prod. 2020;268:121725.

[59] Wang Z, Jiang L, Wang K, Li Y, Zhang G. Novel AgI/$BiSbO_4$ heterojunction for efficient photocatalytic degradation of organic pollutants under visible light: interfacial electron transfer pathway, DFT calculation and degradation mechanism study. J Hazard Mater. 2021;410:124948.

[60] Dasineh Khiavi N, Katal R, Kholghi Eshkalak S, Masudy-Panah S, Ramakrishna S, Jiangyong H. Visible light driven heterojunction photocatalyst of CuO–$Cu_2O$ thin films for photocatalytic degradation of organic pollutants. Nanomaterials. 2019;9(7):1011.

[61] Nazim M, Khan AAP, Asiri AM, Kim JH. Exploring rapid photocatalytic degradation of organic pollutants with porous CuO nanosheets: Synthesis, dye removal, and kinetic studies at room temperature. ACS Omega. 2021;6(4):2601–12.

[62] Pauporte T, Rathouský J. Electrodeposited mesoporous ZnO thin films as efficient photocatalysts for the degradation of dye pollutants. J Phys Chem C. 2007;111(21):7639–44.

[63] Chowdhury ZZ. Preparation, characterization and adsorption studies of heavy metals onto activated adsorbent materials derived from agricultural residues. Thesis. University of Malaya; 2013.

[64] Hoffmann MR, Martin ST, Choi W, Bahnemann DW. Environmental applications of semiconductor photocatalysis. Chem Rev. 1995;95(1):69–96.

[65] Rajendran S, Khan MM, Gracia F, Qin J, Gupta VK. Arumainathan SJSr. $Ce^{3+}$-ion-induced visible-light photocatalytic degradation and electrochemical activity of ZnO/$CeO_2$ nanocomposite. Sci Rep. 2016;6(1):31641.

[66] Fujishima A, Honda K. Electrochemical photolysis of water at a semiconductor electrode. Nature. 1972;238(5358):37–8.

[67] Ollis DF. Contaminant degradation in water. Environ Sci Technol. 1985;19(6):480–4.

[68] Ollis DF, Turchi CS. Heterogeneous photocatalysis for water purification: Contaminant mineralization kinetics and elementary reactor analysis. Environ Prog. 1990;9229–34.

[69] Herrmann J-M. Heterogeneous photocatalysis: fundamentals and applications to the removal of various types of aqueous pollutants. Catal Today. 1999;53(1):115–29.

[70] Antonopoulou M, Kosma C, Albanis T, Konstantinou I. An overview of homogeneous and heterogeneous photocatalysis applications for the removal of pharmaceutical compounds from real

or synthetic hospital wastewaters under lab or pilot scale. Sci Total Env. 2021;765:144163.

[71] Ayodhya D, Veerabhadram G. A review on recent advances in photodegradation of dyes using doped and heterojunction based semiconductor metal sulfide nanostructures for environmental protection. Mater Today Energy. 2018;9:83–113.

[72] Litter MI. Heterogeneous photocatalysis: transition metal ions in photocatalytic systems. Appl Catal B: Environ. 1999;23(2–3):89–114.

[73] Mills A, Davies RH, Worsley D. Water purification by semiconductor photocatalysis. Chem Soc Rev. 1993;22(6):417–25.

[74] Ong W-J, Tan L-L, Ng YH, Yong S-T, Chai S-P. Graphitic carbon nitride (g-$C_3N_4$)-based photocatalysts for artificial photosynthesis and environmental remediation: are we a step closer to achieving sustainability? Chem Rev. 2016;116(12):7159–329.

[75] Kapoor R, Lim K. The impact of acquisitions on the innovation performance of inventors at semiconductor companies. Valhalla, NY, USA: Academy of Management; 2005.

[76] Linsebigler AL, Lu G, Yates Jr, JT. Photocatalysis on $TiO_2$ surfaces: principles, mechanisms, and selected results. Chem Rev. 1995;95(3):735–58.

[77] Smalley JF, Feldberg SW, Chidsey CE, Linford MR, Newton MD, Liu Y-P. The kinetics of electron transfer through ferrocene-terminated alkanethiol monolayers on gold. J Phys Chem. 1995;99(35):13141–9.

[78] Ramesh M, Palanikumar K, Reddy KH. Comparative evaluation on properties of hybrid glass fiber-sisal/jute reinforced epoxy composites. Procedia Eng. 2013;51:745–50.

[79] Behnajady M, Modirshahla N, Hamzavi R. Kinetic study on photocatalytic degradation of CI Acid Yellow 23 by ZnO photocatalyst. J Hazard Mater. 2006;133(1–3):226–32.

[80] Ajmal A, Majeed I, Malik R, Iqbal M, Nadeem MA, Hussain I, et al. Photocatalytic degradation of textile dyes on Cu2O-CuO/TiO2 anatase powders. J Environ Chem Eng. 2016;4(2):2138–46.

[81] Khan MM, Pradhan D, Sohn Y. Nanocomposites for visible light-induced photocatalysis. Cham, Switzerland: Springer; 2017.

[82] Jiang Z, Wang H, Huang H, Cao C. Photocatalysis enhancement by electric field: $TiO_2$ thin film for degradation of dye X-3B. Chemosphere. 2004;56(5):503–8.

[83] Daneshvar N, Salari D, Khataee A. Photocatalytic degradation of azo dye acid red 14 in water: investigation of the effect of operational parameters. J Photochem Photobiol A: Chem. 2003;157(1):111–6.

[84] Alinsafi A, Evenou F, Abdulkarim E, Pons M-N, Zahraa O, Benhammou A, et al. Treatment of textile industry wastewater by supported photocatalysis. Dye Pigment. 2007;74(2):439–45.

[85] Colmenares JC, Luque R. Heterogeneous photocatalytic nanomaterials: prospects and challenges in selective transformations of biomass-derived compounds. Chem Soc Rev. 2014;43(3):765–78.

[86] Wang H, Zhang L, Chen Z, Hu J, Li S, Wang Z, et al. Semiconductor heterojunction photocatalysts: design, construction, and photocatalytic performances. Chem Soc Rev. 2014;43(15):5234–44.

[87] Gouvea CA, Wypych F, Moraes SG, Duran N, Nagata N, Peralta-Zamora P. Semiconductor-assisted photocatalytic degradation of reactive dyes in aqueous solution. Chemosphere. 2000;40(4):433–40.

[88] Salem MA, Shaban SY, Ismail SM. Photocatalytic degradation of acid green 25 using ZnO and natural sunlight. Int J Emerg Technol Adv Eng. 2015;5:439.

[89] Sathya M, Selvan G, Karunakaran M, Kasirajan K, Usha S, Logitha M, et al. Synthesis and characterization of cadmium doped on ZnO thin films prepared by SILAR method for photocatalytic degradation properties of MB under UV irradiation. Eur Phys J Plus. 2023;138(1):1–12.

[90] Mishra S, Tripathi RM, Sinha OP. Recent Developments in Detoxification of Organic Pollutants Using CdS-based Nanocomposites. Nano Biomed Eng. 2021;13(2);95–108.

[91] Liu X, Sayed M, Bie C, Cheng B, Hu B, Yu J, et al. Hollow CdS-based photocatalysts. J Materiomics. 2021;7(3):419–39.

[92] Pasini SM, Valerio A, Yin G, Wang J, de Souza SMGU, Hotza D, et al. An overview on nanostructured $TiO_2$–containing fibers for photocatalytic degradation of organic pollutants in wastewater treatment. J Water Process Eng. 2021;40:101827.

[93] Sharma K, Raizada P, Hasija V, Singh P, Bajpai A, Nguyen V-H, et al. ZnS-based quantum dots as photocatalysts for water purification. J Water Process Eng. 2021;43:102217.

[94] Rani V, Sharma A, Kumar A, Singh P, Thakur S, Singh A, et al. $ZrO_2$-based photocatalysts for wastewater treatment: from novel modification strategies to mechanistic insights. Catalysts. 2022;12(11):1418.

[95] Madaan V, Mohan B, Bhankar V, Ranga R, Kumari P, Singh P, et al. Metal-decorated $CeO_2$ nanomaterials for photocatalytic degradation of organic pollutants. Inorg Chem Commun. 2022;146:110099.

[96] Okla MK, Harini G, Dawoud TM, Akshhayya C, Mohebaldin A, AL-ghamdi AA, et al. Fabrication of $MnFe_2O_4$ spheres modified $CeO_2$ nano-flakes for sustainable photodegradation of MB dye and antimicrobial activity: A brief computational investigation on reactive sites and degradation pathway. Colloids Surf A: Physicochem Eng Asp. 2022;641:128566.

[97] Fauzi A, Jalil A, Hassan N, Aziz F, Azami M, Hussain I, et al. A critical review on relationship of $CeO_2$-based photocatalyst towards mechanistic degradation of organic pollutant. Chemosphere. 2022;286:131651.

[98] Zhang L, Webster TJ. Nanotechnology and nanomaterials: promises for improved tissue regeneration. Nano today. 2009;4(1):66–80.

[99] Shi L, Lin H. Preparation of band gap tunable $SnO_2$ nanotubes and their ethanol sensing properties. Langmuir. 2011;27(7):3977–81.

[100] Naeem H, Tofil HM, Soliman M, Hai A, Zaidi SHH, Kizilbash N, et al. Reduced graphene oxide-zinc sulfide nanocomposite decorated with silver nanoparticles for wastewater treatment by adsorption, photocatalysis and antimicrobial action. Molecules. 2023;28(3):926.

[101] Gherbi B, Laouini SE, Meneceur S, Bouafia A, Hemmami H, Tedjani ML, et al. Effect of pH value on the bandgap energy and particles size for biosynthesis of ZnO nanoparticles: Efficiency for photocatalytic adsorption of methyl orange. Sustainability. 2022;14(18):11300.

[102] Kanakaraju D, Chandrasekaran A. Recent advances in $TiO_2$/ZnS-based binary and ternary photocatalysts for the degradation of organic pollutants. Sci Total Env. 2023;868:161525.

[103] Assadullah I, Bhat AA, Malik JH, Malik KA, Tomar R, Khandy SA. Electronic structure, optical, photocatalytic and charge storage performance of $WO_3$ nanostructures. J Phys Chem Solids. 2022;165:110649.

[104] Mahmoud ZH, AL-Bayati RA, Khadom AA. Modified anatase phase of $TiO_2$ by WO3 nanoparticles: Structural, morphology and spectral evaluations. Mater Today: Proc. 2022;61:799–804.

[105] Munawar T, Mukhtar F, Nadeem MS, Manzoor S, Ashiq MN, Mahmood K, et al. Fabrication of dual Z-scheme $TiO_2$-$WO_3$-$CeO_2$ heterostructured nanocomposite with enhanced photocatalysis, antibacterial, and electrochemical performance. J Alloy Compd. 2022;898:162779.

[106] Alimohammadi E, Mahdikhah V, Sheibani S. Type-II band alignment in CNT-modified $SrTiO_3$-$Fe_2TiO_5$ heterostructure nanocomposite for photocatalytic degradation of organic dyes. Appl Surf Sci. 2022;598:153816.

[107] Zhou E, Raulot J-M, Xu H, Hao H, Shen Z, Liu H. Structural, electronic, and optical properties of rare-earth-doped $SrTiO_3$ perovskite: A first-principles study. Phys B: Condens Matter. 2022;643:414160.

[108] Balestra L, Reggiani S, Gnani E, Gnudi A. Group velocity of electrons in 4H-SiC from density functional theory simulations. Solid·State Electron. 2022;194:108338.

[109] Yang L, Wang J, Zhang Y, Zhou B, Tan P, Pan J. Construction of S-scheme BiOCl/CdS composite for enhanced photocatalytic degradation of antibiotic. J Mater Sci: Mater Electron. 2022;33(16):13303–15.

[110] Fatimah I, Purwiandono G, Hidayat A, Sagadevan S, Kamari A. Mechanistic insight into the adsorption and photocatalytic activity of a magnetically separable γ-$Fe_2O_3$/Montmorillonite nanocomposite for rhodamine B removal. Chem Phys Lett. 2022;792:139410.

[111] Assali S, Zardo I, Plissard S, Kriegner D, Verheijen M, Bauer G, et al. Direct band gap wurtzite gallium phosphide nanowires. Nano Lett. 2013;13(4):1559–63.

[112] Nisham Rosly H, Doroody C, Harif MN, Mohamad IS, Isah M, Amin N. Optoelectrical properties of treated CdSe thin films with variations in indium chloride concentration. materials. 2023;16(11):4108.

[113] Ray S, Tarafder K. Investigation of CdSe and ZnSe as potential back surface field layers for CdTe-based solar cells: A study from first principles calculations. Adv Theory Simul. 2023;6(3):2200718.

[114] Jiang X, Tan H, Shi X, Cheng X, Hu W, Hu X. Preparation of $Bi_2O_3$/BiOI step-scheme heterojunction photocatalysts and their degradation mechanism of methylene blue. J Wuhan Univ Technol-Mater Sci Ed. 2022;37(5):801–6.

[115] Rajan KD, Srinivasan D, Gotipamul PP, Khanna S, Chidambaram S, Rathinam M. Design of a novel $ZnBi_2O_4$/$Bi_2O_3$ type-II photo-catalyst via short term hydrothermal for enhanced degradation of organic pollutants. Mater Sci Eng: B. 2022;285:115929.

[116] Zhang X, Wang J, Dong X-X, Lv Y-K. Functionalized metal-organic frameworks for photocatalytic degradation of organic pollutants in environment. Chemosphere. 2020;242:125144.

[117] Ariga K, Shrestha LK. Zero-to-one (or more) nanoarchitectonics: How to produce functional materials from zero-dimensional single-element unit, fullerene. Mater Adv. 2021;2(2):582–97.

[118] Jin Y, Yi Y, Yeung B. Mass spectrometric analysis of protein deamidation–A focus on top-down and middle-down mass spectrometry. Methods. 2022;200:58–66.

[119] Kelleher NL, Lin HY, Valaskovic GA, Aaserud DJ, Fridriksson EK, McLafferty FW. Top down versus bottom up protein characterization by tandem high-resolution mass spectrometry. J Am Chem Soc. 1999;121(4):806–12.

[120] Khan Y, Sadia H, Ali Shah SZ, Khan MN, Shah AA, Ullah N, et al. Classification, synthetic, and characterization approaches to nanoparticles, and their applications in various fields of nanotechnology: a review. Catalysts. 2022;12(11):1386.

[121] Guo Y, Xu K, Wu C, Zhao J, Xie Y. Surface chemical-modification for engineering the intrinsic physical properties of inorganic two-dimensional nanomaterials. Chem Soc Rev. 2015;44(3):637–46.

[122] Kim HY, Jun M, Lee K, Joo SH. Skeletal nanostructures promoting electrocatalytic reactions with three-dimensional frameworks. ACS Catal. 2022;13:355–74.

[123] Getahun YW, Gardea-Torresdey J, Manciu FS, Li X, El-Gendy AA. Green synthesized superparamagnetic iron oxide nanoparticles for water treatment with alternative recyclability. J Mol Liq. 2022;356:118983.

[124] Mahdavi Dehkharghani F, Ghahremanlou M, Zandi Z, Jalili M, Mozafari M, Mardani P. Future energy and therapeutic perspectives of green nano-technology: recent advances and challenges. Nano Micro Biosyst. 2023;2(1):11–21.

[125] Hammami I, Alabdallah NM. Gold nanoparticles: Synthesis properties and applications. J King Saud Univ-Sci. 2021;33(7):101560.

[126] Polavarapu L, Nickel B, Feldmann J, Urban AS. Advances in quantum-confined perovskite nanocrystals for optoelectronics. Adv Energy Mater. 2017;7(16):1700267.

[127] Ananthakumar S, Babu SM. Progress on synthesis and applications of hybrid perovskite semiconductor nanomaterials – A review. Synth Met. 2018;246:64–95.

[128] Samadi M, Zirak M, Naseri A, Kheirabadi M, Ebrahimi M, Moshfegh AZ. Design and tailoring of one-dimensional ZnO nanomaterials for photocatalytic degradation of organic dyes: a review. Res Chem Intermed. 2019;45:2197–254.

[129] Chenab KK, Sohrabi B, Jafari A, Ramakrishna S. Water treatment: functional nanomaterials and applications from adsorption to photodegradation. Mater Today Chem. 2020;16:100262.

[130] Ajormal F, Moradnia F, Taghavi Fardood S, Ramazani A. Zinc ferrite nanoparticles in photo-degradation of dye: mini-review. Chem Rev. 2020;2(2):90–102.

[131] Rauf M, Ashraf SS. Fundamental principles and application of heterogeneous photocatalytic degradation of dyes in solution. Chem Eng J. 2009;151(1–3):10–8.

[132] Kim SB, Hong SC. Kinetic study for photocatalytic degradation of volatile organic compounds in air using thin film $TiO_2$ photocatalyst. Appl Catal B: Environ. 2002;35(4):305–15.

[133] Shaikh SMF, Rahman G, Mane RS, Joo O-S. Bismuth oxide nanoplates-based efficient DSSCs: Influence of ZnO surface passivation layer. Electrochim Acta. 2013;111:593–600.

[134] Tomar R, Abdala AA, Chaudhary R, Singh N. Photocatalytic degradation of dyes by nanomaterials. Mater Today: Proc. 2020;29:967–73.

[135] Hosseini SA, Saeedi R. Photocatalytic degradation of rhodamine B by nano bismuth oxide: Process modeling by response surface methodology (RSM). 2017;37–46.

[136] Jamali-Sheini F, Yousefi R, Bakr NA, Cheraghizade M, Sookhakian M, Huang NM. Highly efficient photo-degradation of methyl blue and band gap shift of SnS nanoparticles under different sonication frequencies. Mater Sci Semicond Process. 2015;32:172–8.

[137] Chen C, Lu C, Chung Y, Jan J. UV light induced photodegradation of malachite green on $TiO_2$ nanoparticles. J Hazard Mater. 2007;141(3):520–8.

[138] Qutub N, Pirzada BM, Umar K, Sabir S. Synthesis of CdS nanoparticles using different sulfide ion precursors: formation mechanism and photocatalytic degradation of Acid Blue-29. J Environ Chem Eng. 2016;4(1):808–17.

[139] Chandran P, Kumari P, Khan SS. Photocatalytic activation of CdS NPs under visible light for environmental cleanup and disinfection. Sol energy. 2014;105:542–7.

[140] Jan FA, Ullah R, Shah U, Saleem M, Ullah N. Band gap tuning of zinc oxide nanoparticles by the addition of (1-4%) strontium. Synthesis, characterization of the catalyst and its use for the photocatalytic degradation of acid violet-17 dye in aqueous solution. Environ Eng Manag J. 2020;19(11):2039–48.

[141] Zeng Q, Liu Y, Shen L, Lin H, Yu W, Xu Y, et al. Facile preparation of recyclable magnetic Ni@ filter paper composite materials for efficient photocatalytic degradation of methyl orange. J Colloid Interface Sci. 2021;582:291–300.

[142] Hunge Y, Yadav A, Khan S, Takagi K, Suzuki N, Teshima K, et al. Photocatalytic degradation of bisphenol A using titanium dioxide@ nanodiamond composites under UV light illumination. J Colloid Interface Sci. 2021;582:1058–66.

[143] Mohamed A, Ghobara MM, Abdelmaksoud M, Mohamed GG. A novel and highly efficient photocatalytic degradation of malachite green dye via surface modified polyacrylonitrile nanofibers/biogenic silica composite nanofibers. Sep Purif Technol. 2019;210:935–42.

[144] Alamelu K, Raja V, Shiamala L, Ali BJ. Biphasic $TiO_2$ nanoparticles decorated graphene nanosheets for visible light driven photocatalytic degradation of organic dyes. Appl Surf Sci. 2018;430:145–54.

[145] Atchudan R, Edison TNJI, Perumal S, Vinodh R, Lee YR. In-situ green synthesis of nitrogen-doped carbon dots for bioimaging and $TiO_2$ nanoparticles@ nitrogen-doped carbon composite for photocatalytic degradation of organic pollutants. J Alloy Compd. 2018;766:12–24.

[146] Zhao G, Liu L, Li C, Zhang T, Yan T, Yu J, et al. Construction of diatomite/ZnFe layered double hydroxides hybrid composites for enhanced photocatalytic degradation of organic pollutants. J Photochem Photobiol A: Chem. 2018;367:302–11.

[147] Zouhier M, Tanji K, Navio J, Hidalgo M, Jaramillo-Páez C, Kherbeche A. Preparation of $ZnFe_2O_4$/ZnO composite: effect of operational parameters for photocatalytic degradation of dyes under UV and visible illumination. J Photochem Photobiol A: Chem. 2020;390:112305.

[148] Liu W, Huang F, Liao Y, Zhang J, Ren G, Zhuang Z, et al. Treatment of CrVI-containing Mg(OH)2 nanowaste. Angew Chem. 2008;47(30):5619–22.

[149] Chen Z, Ma T, Li Z, Zhu W, Li L. Enhanced photocatalytic performance of S-scheme CdMoO4/CdO nanosphere photocatalyst. J Mater Sci Technol. 2024;179:198–207.

[150] He H, Wan Q, Hou Z, Zhou Q, Wang L. Organoelectrophotocatalytic generation of acyl radicals from formamides and aldehydes: access to acylated 3-CF3-2-oxindoles. Org Lett. 2024;25(38):7014–9.

[151] Ma J, Li J, Weng L, Ouyang X, Chen Y, Li Y. Phosphorus-enhanced and calcium-retarded transport of ferrihydrite colloid: mechanism of electrostatic potential changes regulated via adsorption speciation. Environ Sci Technol. 2023;57(10):4219–30.

[152] Li H, Wu Y, Xu Z, Wang Y. *In situ* anchoring Cu nanoclusters on Cu-MOF: A new strategy for a combination of catalysis and fluorescence toward the detection of $H_2O_2$ and 2,4-DNP. Chem Eng J. 2023;479:147508. doi: 10.1016/j.cej.2023.147508

[153] Li H, Xu X, Liu Y, Hao Y, Xu Z. Fluorophore molecule loaded in Tb-MOF for dual-channel fluorescence chemosensor for consecutive visual detection of bacterial spores and dichromate anion. J Alloy Compd. 2023;944:169138.

[154] Chen D, Wang Q, Li Y, Li Y, Zhou H, Fan Y. A general linear free energy relationship for predicting partition coefficients of neutral organic compounds. Chemosphere. 2020;247:125869.

[155] Li H, Wang Y, Jiang F, Li M, Xu Z. A dual-function [Ru(bpy)3]2+ encapsulated metal organic framework for ratiometric Al3+ detection and anticounterfeiting application. Dalton Trans. 2023;52(12):3846–54.

[156] Zheng Y, Liu Y, Guo X, Chen Z, Zhang W, Wang Y, et al. Sulfur-doped g-C3N4/rGO porous nanosheets for highly efficient photocatalytic degradation of refractory contaminants. J Mater Sci Technol. 2020;41(2020):117–26.

[157] Wang Z, Chen C, Liu H, Hrynshpan D, Savitskaya T, Chen J, et al. Enhanced denitrification performance of Alcaligenes sp. TB by Pd stimulating to produce membrane adaptation mechanism coupled with nanoscale zero-valent iron. Sci Total Environ. 2020;708:135063.

[158] Kong L, Liu Y, Dong L, Zhang L, Qiao L, Wang W, et al. Enhanced red luminescence in CaAl12O19:Mn4+via doping Ga3+ for plant growth lighting. Dalton Trans. 2020;49(6):1947–54.